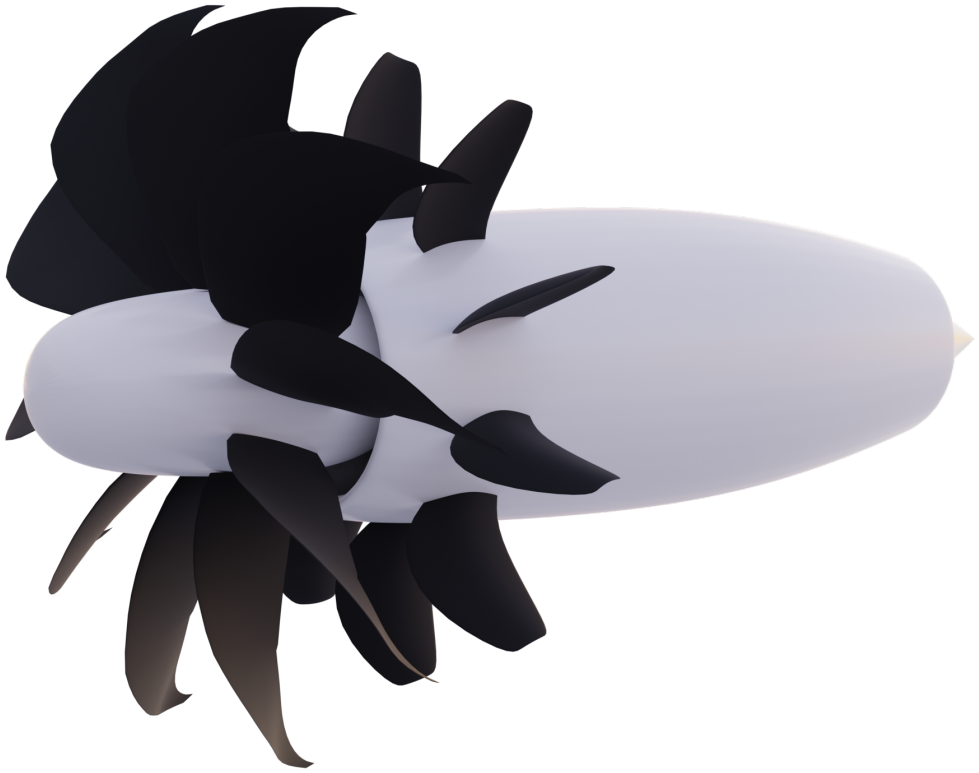

Off-Design Performance Modelling of a Propfan Aero Engine

An off-design performance evaluation of a notional engine design for future reductions in fuel consumption and emissions

Master's thesis in Applied Mechanics and Mobility Engineering

David Hanås
Frowin Winkes

DEPARTMENT OF MECHANICS AND MARITIME SCIENCES
CHALMERS UNIVERSITY OF TECHNOLOGY
Gothenburg, Sweden 2023
www.chalmers.se

Master's thesis 2023

Off-Design Performance Modelling of a Propfan Aero Engine

An off-design performance evaluation of a notional engine design for future reductions in fuel consumption and emissions

DAVID HANÅS
FROWIN WINKES

CHALMERS
UNIVERSITY OF TECHNOLOGY

Department of Mechanics and Maritime Sciences
Division of Fluid Dynamics
Chalmers University of Technology
Gothenburg, Sweden 2023

Off-Design Performance Modelling of a Propfan Aero Engine
An off-design performance evaluation of a notional engine design for future reductions in fuel consumption and emissions

Supervisor: Eric Blidmark, Engine Performance Research Engineer, GKN Aerospace Sweden AB
Examiner: Carlos Xisto, Associate professor at Mechanics and Maritime Sciences, Division of Fluid Dynamics

Master's Thesis 2023
Department of Mechanics and Maritime Sciences
Division of Fluid Dynamics
Chalmers University of Technology
SE-412 96 Gothenburg
Telephone +46 31 772 1000

Cover: Propfan Concept Render by Frowin Winkes.

Typeset in LaTeX
Printed by Chalmers Reproservice
Gothenburg, Sweden 2023

Abstract

The following report covers the methodology behind creating an off-design model for an existing notional propfan engine model in NPSS. Particular attention has been given to; the creation and implementation of a custom propeller element together with the relevant performance maps, ensuring operability throughout the flight envelope, proposition of thrust ratings and their accompanying scheduling strategies as well as performing whole mission envelope simulations in NPSS in order to quickly evaluate a notional engine throughout its range of operations. From this a recommendation for how a future propfan engine could be controlled has been given along with some observations and conclusions on SFC, bleed work and operability.

Keywords: propfan, notional engine, NPSS, aerospace, sustainable aviation, net zero, IATA 2050.

Acknowledgements

We would like to take this opportunity to express our appreciation to several individuals who have been essential for a successful completion for this thesis project. Firstly we would like to thank Alexandre Capitao Patrao for kindly allowing us access to his tool Optoprop, which has proven to be an essential part of our research.

Additionally, we also would like to express our appreciation to Eric Blidmark, our supervisor at GKN Aerospace, for his support and direction. Eric's knowledge, perspective, insight and feedback have been invaluable in helping us facing new challenges and overcoming obstacles. We also want to express our gratitude to the other members of the department of Future Concepts at GKN Aerospace Trollhättan. Their suggestions and ideas have been helpful in assisting us in improving and accomplishing our objectives.

Carlos Xisto is also to be recognised and thanked for acting as our examiner. His advice and feedback have been helpful in improving our work and making sure it is of the best calibre.

A special thanks to our desk mates Elias Chalhoub and August Skoglund who have been good moral support and given good feedback on all our graphs along the way.

Finally, we want to thank our families and friends from the bottom of our hearts for their continuous support and inspiration during this journey.

David Hanås & Frowin Winkes, Gothenburg, June 2023

List of Acronyms

Below is the list of acronyms that have been used throughout this thesis listed in alphabetical order:

BPR	By Pass Ratio
CRZ	Cruise
EGT	Exhaust Gas Temperature
HPC	High Pressure Compressor
HPT	High Pressure Turbine
IATA	International Air Transport Association
IC	Initial Climb
IDE	Integrated Development Environment
IGV	Inlet Guide Vanes
LE	Leading Edge
IPC	Intermediate Pressure Compressor
LPC	Low Pressure Compressor
LPT	Low Pressure Turbine
MTOW	Max Take Off Weight
NASA	National Aeronautics and Space Administration
NPSS	Numerical Propulsion System Simulation
OAT	Outside Air Temperature
OGV	Outlet Guide Vanes
OOP	Object Oriented Programming
PLA	Power Lever Angle
SFC	Specific Fuel Consumption
SMN	Stall margin (constant speed)
SRV	Swirl Recovery Vane
SwRI	Southwest Research Institutes
TET	Turbine Entry Temperature
TO	Take off
TOC	Top of climb
TOEoR	Take Off End of Runway
TOGA	Take off go around
UDF	Un-ducted Fan
WV	Wolverine Ventures

Nomenclature

β	Blade element pitch angle
Δv	Incremental induced axial velocity behind the disk
$\dot{m}$	Mass flow
$\eta_{overall}$	Overall efficiency
η_{prop}	Propulsive efficiency
μ	LE sweep angle
ρ	Air Density
Θ	Swirl angle downstream of the propeller blades
A	Area
a	1ISA sonic airspeed
A_P	Area of the propeller disc
C_P	Coefficient of power
C_T	Coefficient of Thrust
D	Diameter
F_N	Total net thrust
h	enthalpy
HTR	Hub to tip ratio
J	Advance ratio of the propeller
$M_{freestream}$	Freestream Mach number
M_{rel}	Relative Mach number
n	Rotational speed
p_s	Pressure, static
p_t	Pressure, total
p_{inf}	Ambient pressure
P_{prop}	Power to the propeller
r	Radius
r_i	Radius at given node indexed by i
T	Thrust
TAS	True air speed
U_{tip}	Speed of the tip
v_P	Velocity of fluid downstream propeller
v_S	Velocity of fluid in the slipstream
v_{inf}	Ambient velocity of fluid
w	Angular velocity
W	mass flow used in NPSS
$x_{rel,offset}$	relative offset in x

Contents

List of Figures

List of Tables

1
Introduction

1.1 Background

As the aeronautical industry aims to reach net zero by 2050 [1], different concepts are being studied that aim to reduce CO2, NOX, particulate emissions and reduced fuel consumption. The reduction of fuel consumption can be done by either increasing the thermal efficiency, or the propulsive efficiency. Looking at the equation below one can see that the propulsive efficiency can be increased by decreasing the jet velocity which, if a constant thrust is to be maintained, requires an increase in masss flow. This gives that a propeller or fan with a large diameter and slow rotational speed has higher propulsive efficiency than a smaller one, spinning at higher rotational speed.

$$\eta_{prop} = \frac{2}{1 + \frac{v_j}{v_0}}$$
$$v_j = Jetspeed$$
$$v_0 = Flightspeed$$

One concept to increase the efficiency of the aero engine is the propfan concept, which has some advantages over the common ducted turbofan. While the traditional ducted turbofan is starting to reach its size limit, the propfan concept allows higher efficiency through a radical increase in bypass ratio. Further, Larsson et al. [2] writes that the propfan can have a larger diameter than the turbofan with less increase in drag and weight penalties, compared to the turbofan, because of the lack of a nacelle.

An aero engine is often designed at one operating condition, for civil engines this is usually Top of Climb (TOC), but must be able to run off-design in the whole flight envelope under varying conditions and thrust settings, so-called ratings. These ratings require control schedules of key engine parameters which are the objective of this thesis.

1.2 Historical Perspective

The design of a propfan has been a hot topic previously. During the 70-80s when oil prices were high, a lot of research was done in the field of profan engines as they, for

the same reasons as today, promised a more efficient alternative to the turbofan engines in use [3]. These studies were conducted by a range of different companies and institutions, some examples includes NASA, General Electric (GE), and Hamilton Standard [4]. During this time there have been several different designs of propfans, both as counter rotating and as single rotor, with and without swirl recovery vanes (SRV) and single rotor with gearbox and pitch control [5]. The NASA funded research on high speed propellers in connection to these projects is still to this day one of the larger studies made on propeller performance. Some of the research done concludes the propfan or advanced turboprop propulsion system to have superior characteristics to a turbofan as early as 1990s [6].

The progress made in these projects varied greatly, some were just ideas and concept, but a few of them made it to the flight test phase. Examples of these are the GE36 (part of the UDF project) and the PW-Allison 578-DX, tested on a demonstrator MD-80 [7]. These two engine concepts are quite similar, both having a pusher setup with counter rotating blades. Unfortunately the UDF project got cancelled in the late 1980s but some of the advancements made during the project were carried over to other projects, one such example were the composite fan blades [8]. The same tragedy followed with other propfan projects getting cancelled in the early 1990s as well.

Now once again with rising fuel prices and an initiative from IATA for net zero in 2050, the need for highly fuel efficient engines is high. This leads to old ideas and concepts being revisited, such as the propfan.

1.3 Aim

This work investigates off-design performance points of a porpfan aero-engine model. The main goal was to establish suitable propeller/propfan maps, optimize the split of air flow, develop a control strategy for fuel flow and pitch, and simulating these with the help of NPSS in a typical flight mission envelope. The thrust control included both variable blade pitch coupled with swirl loss recovery through swirl recovery vanes and fuel flow, contrary to a turbofan which more often, in simple models, only uses fuel flow to control thrust. The required thrust was given by an existing mission profile and known ratings for engines of similar size. Similarly, temperature limits, shaft speeds and other limiting specifications were assumed to be similar to existing engines of similar size. Running the simulation at decreased throttle was looked into and followed a similar strategy as stated in [9].

The strategies, methods and tools developed during the project may be applicable to other engine architectures since one of the goals during the project was to find suitable methodology for establishing engine thrust ratings and develop control schedules in general. These are later verified by running the model through a specified typical mission and sweeping through the envelope (i.e. Start, take-off, climb, cruise, descent, landing) and compared to existing data.

1.4 Limitations

Due to the large scope of the project, some limitations had to be set in place in order to finish before the set deadlines. The work done only looked at the performance and implementations of civil engines and strategies, implementations of non-civil character were not included or looked at. This project did not focus on compressor and turbine maps and the performance of the internal design. Particularly the work used existing maps that were deemed to be a good approximation. An effort was made into developing off-design propeller maps with the use of Optoprop which were used to extend existing propeller performance maps based upon "known-good" data from previous research [10]. The effect of the swirl recovery vanes (SRV) was also looked at and taken into account in the form of an efficiency increase as done by Larsson in [2]. The thrust requirements were not looked at in depth and as such values from a similar engine design and mission profile were used. The thrust ratings and control strategies were not intended to be fully optimized as it would be too time-consuming to do so. Instead, the work was focused on methodology and performance trends rather than numerical results. Finally, no book keeping of emissions or environmental impact was performed and all simulation cases looked at steady state conditions.

1.5 Description of the Model

The engine model in NPSS follows a typical layout for an aero engine. Most noteworthy is the use of a propeller with variable blade pitch that is powered by the low pressure turbine and acts on a common shaft with the LPC and IPC, this will be looked at in more detail in the method section. This particular model uses swirl recovery vanes to guide the flow and increase the propulsion system efficiency. The increase in efficiency can be seen with the reduced swirl due to the SRV, in combination with the higher relative axial momentum. The propfan has been modelled similar to a turbofan since the core of this propfan has been assumed to be very similar to a usual turbofan, featuring a high and a low-pressure shaft. A propeller has been attached in a tractor configuration to the low-pressure shaft with a gearbox. The existing design point model is based purely on public information and data and the same holds true for all of the additions made in order to run the model at off-design.

2
Theory

This chapter presents the main theory regarding propellers, aero engines, ratings and mission profile.

2.1 Propeller

This section presents the relevant underlying physics of propellers.

2.1.1 Disc Actuator Theory

The thrust generated by a propeller can be calculated using actuator disc theory [11], sometimes also called momentum theory. This assumes that the flow is incompressible and that any change in pressure and velocity happens instantaneously at the face of the disc. The rotor or propeller is modelled as a disc that is infinitely thin, with infinite amount of blades and the diameter denoted as D. The fluid conditions at the inlet are given by the ambient conditions and are described by the variables P_{inf}, v_{inf} and ρ. The flow through the disc is assumed to be uniform and denoted by v_p, whereas the uniform slipstream of accelerated flow behind the disc is denoted by v_s. This can all be visualized by a stream tube with a control volume surrounding it, as seen in Figure 2.1. Thrust can then be calculated using either momentum change or as a pressure difference on the surfaces of the disc [12].

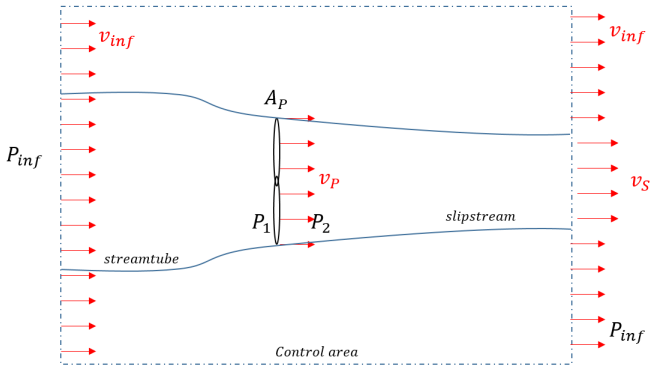

Figure 2.1: Disc Actuator Theory Model

The thrust can then be described as a force acting on the surface of the disc, or as a change in momentum:

$$T = (P_2 - P_1) \cdot A_p \tag{2.1}$$

$$T = \rho \cdot v_p \cdot A_p \cdot (v_s - v_{inf}) \tag{2.2}$$

The advance ratio is one of the most important variables when it comes to propeller performance. It is mathematically defined as seen in equation 4 and can conceptually be thought of as the distance the propeller tip travels, relative to the circumference of the propeller disc, for each revolution (see Figure 2.2). This leads to the advance ratio (J) decreasing for higher rotational speed and/or lower ambient velocities and increasing for lower rotational speed and/or higher ambient velocities. The advance ratio can be calculated by the inlet velocity, v_{inf} the rotational speed n, and the diameter D as in equation 2.3

$$J = \frac{V_{inf}}{n \cdot D} \tag{2.3}$$

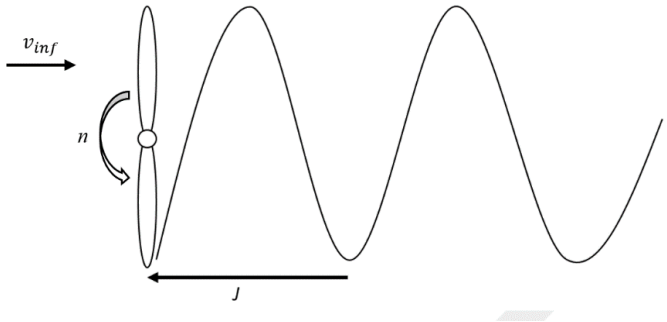

Figure 2.2: Illustration of advance ratio for a propeller

C_T, thrust coefficient, and C_P, power coefficient, are non-dimensional descriptions of the produced thrust and power required by the propeller. The coefficients are obtained by the equations 2.4 and 2.5. Here, ρ denotes the density of the fluid and P denotes the shaft power in other words the product of rotational speed and torque.

$$C_T = \frac{T}{\rho \cdot n^2 \cdot D^4} \tag{2.4}$$

$$C_P = \frac{P}{\rho \cdot n^3 \cdot D^5} \tag{2.5}$$

The propeller performance can be defined either by thrust and power, or as their non-dimensional part coefficient of power and coefficient of thrust. These combined with the advance ratio, J, can be used to calculate the efficiency as in equation 2.6. [2], [12].

$$\eta_{prop} = \frac{T \cdot v_{inf}}{P} = \frac{C_T \cdot J}{C_P} \tag{2.6}$$

The diameter and shaft power can then be used to calculate the total disc loading (see equation 2.7). The disc loading can be used to directly size a propeller if the designer knows the maximum allowable disc loading for a given propeller design.

$$DiscLoading = \frac{P}{D^2} \tag{2.7}$$

2.1.2 Blade Pitch

The angle of the propeller blade relative to the plane of rotation for the propeller is commonly referred to as blade pitch. Similar to the incidence angle on aircraft this angle is relative to the "forward" direction of the air foil. Since the relative incoming velocity changes both in magnitude and direction along the radius of a propeller, the optimal pitch angle will vary radially too.

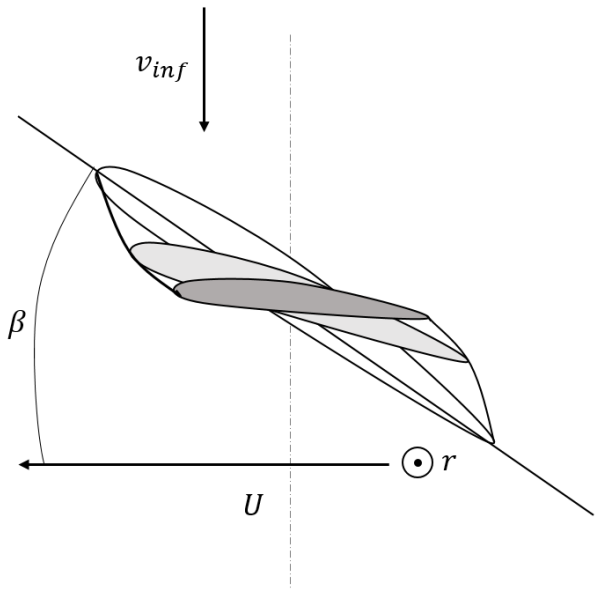

Figure 2.3: Illustration of blade pitch as seen when looking radially onto a propeller blade

2.1.3 Swirl Loss and Recovery

For a given propeller design, blade pitch and rotational speed there is a certain amount of air that is turned by the propeller blades which leads to a rotating flow in the wake of the propeller. Since this flow is not in the axial direction it does not contribute to the overall thrust of the propeller, even though energy has been expended in the propeller to induce this motion. Thus this swirling motion becomes the source for one of the loss factors that has to be considered in propeller design, this loss in particular is usually referred to as swirl loss.

The swirl losses can be a significant portion of the losses for a propeller at high blade loading such as under take-off conditions [13]. To decrease these losses one might consider a different propeller design with higher efficiency and usually lower blade loading. Since this might not always be possible because of other design constraints such as performance at other conditions or noise, the idea of recovering these losses instead might be more tempting. This can be done with a row of stators behind the propeller known as Swirl Recovery Vanes (SRV). The SRV concept has previously been shown to recover about 40% of the swirl losses generated by a propfan and is suspected to recover even more with further optimisation [13], while still maintaining a good hub choke margin and performance. Similar to the blades of a modern propeller the SRVs can be made variable in pitch in order to perform over a broader range of operational conditions, however the SRV geometry itself will still only be optimal for a very narrow range of conditions.

$$SwirlLoss = \frac{\pi \cdot (1 - HTR^2)}{8} \cdot \frac{J^3 \cdot (\frac{\Delta v}{v_{inf}})^3 \cdot tan^2\Theta}{C_P} \tag{2.8}$$

According to Larsson et al. [2], the swirl losses can be calculated using equation 2.8. The required slip stream characteristics can be either obtained from simulations or in case of experiments, by measuring the flow direction downstream of the propeller.

2.1.4 Wing/Blade Sweep

Wing sweep is a design property commonly used on trans- and supersonic aircraft in order to substantially reduce wave drag and increase the critical Mach for a given wing [14].

An aircraft traveling at speeds sufficiently close to sonic conditions might encounter sonic flows over the wings before the remaining airframe does. This is due to the acceleration of the local flow being caused by the low-pressure regions on the top side of the wings. From this accelerated state the local flow will need to return to freestream conditions and as such an adverse pressure gradient forms, if the flow is at or above sonic conditions this will result in the creation of a shock. According to Raymer, for a well-designed wing this potential shock should be at a constant percentage of the chord as measured from the LE [14].

However, by sweeping the wing the curvature seen over the body by the airflow will decrease as will the magnitude of the accelerating low-pressure regions. This leads to less acceleration and thus a lower local Mach number. If we disregard 3 dimensional effects and the influence an aircraft fuselage might have on this, then an estimation can be computed with equation 2.9.

$$M_{rel} = cos\mu \cdot M_{freestream} \tag{2.9}$$

It should be noted however that sweeping the wing might lead to substantial span wise flows at lower velocities and as such a loss of lift, an effect that is not easily taken into account.

2.1.5 Propeller Maps and Typical Performance Behaviour

Since the performance of a propeller shows some trends that are universal between designs we would like to introduce the reader to these in the following section. As part of this thesis, a significant amount of time was spent on visualising and getting a feel for how the propfan would affect the core and overall engine's performance. A part of this was to understand how much thrust would be reasonable to expect from the propfan and how varying the pitch of the fan blades would impact C_P, efficiency and overall power requirement.

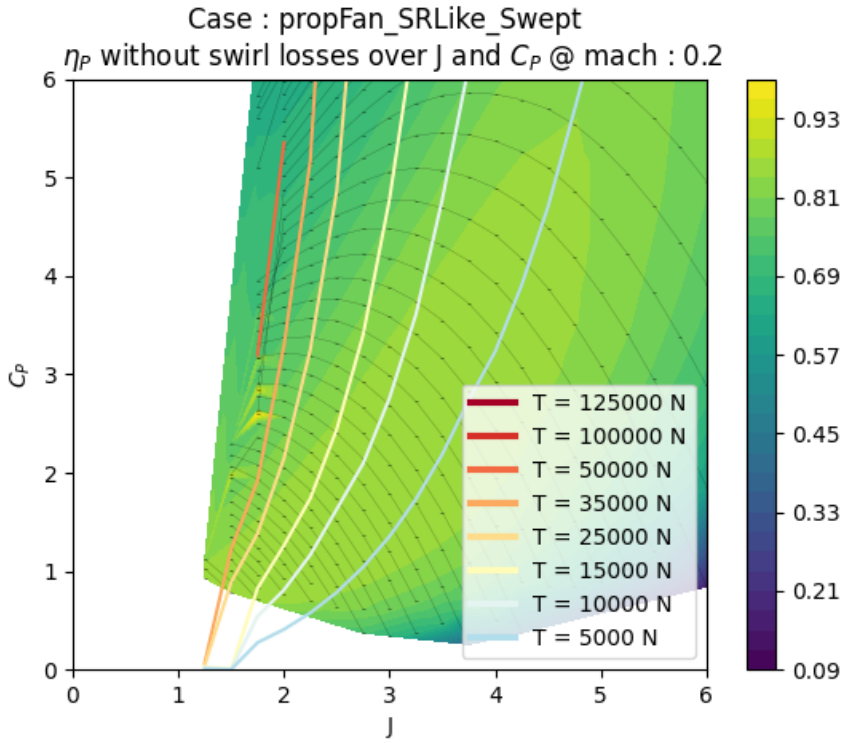

Figure 2.4: Typical propeller efficiency map with isolines for constant thrust and blade pitch plotted

The graph above shows a typical propeller map, in this case computed using Optoprop, and with lines plotted for constant thrust in shades of blue to red and blade pitch in black. In this case higher C_P correspond with larger blade pitch angles. Remember that higher advance ratios (J) lead to lower propeller/fan rpm and/or higher ambient air velocity. Note how there are multiple solutions for any given thrust requirement but how the span of acceptable advance ratios (J) narrows more and more the higher the thrust requirement gets. The blade pitch lines meanwhile run close to perpendicular to the thrust lines for some cases, indicating that changing the blade pitch might not be enough to achieve a wanted thrust as the thrust might not change that much after pitching the blades further than a certain point. The only way to increase thrust in that case would be to increase the fan rpm.

2.2 Turbofans

Turbofans are the main engine type used in long distance air traffic, they are widely used because of their relatively good fuel economy and low noise compared to the thrust generated. The turbofan works by having a core drive a larger fan with high mass flow and low jet velocity. The core is designed with several compressor stages, burner and turbine stages. Modern turbofans have two or three independent shafts, a low speed, a medium and a high speed. Some even have a gear between the low speed shaft and the fan. To get the most efficiency the fan needs to be big, which has some drawbacks in weight and size. The increase in size also means an increase

in nacelle size, which makes further increases weight. This can cause installation problems caused by ground clearance and heavy weight.

2.3 Turboprops

Turboprops are used as aero engines, usually for smaller sized, regional aircraft. The turboprop works by having a gas turbine drive a propeller to generate thrust. It is common for these engines to only a few different spool speeds for the low pressure shaft in order for the propeller to stay at favorable conditions, contrary to turbofans which commonly do not control the spool speed directly. The most common method of controlling the spool speed is to vary the propeller blade pitch. A big disadvantage of turboprops is that they generally only operate up to Mach 0.65 whereas turbofans have cruise speed of Mach 0.8. Turboprops have been used since the 1940's, and have evolved since. Modern turboprops have better fuel consumption to smaller turbofans, but can also have lower overall operation costs. One of the key advantages with a turboprop is their high efficiency at low speed and low altitude making and the ability to operate at short runways. This makes them popular for regional flights with short runways and short overall travel distances.

The design point for an turbofan is usually the top of climb, but some research suggests that an engine with a propeller might have problems with achieving take-off thrust unless designed for take-off, thus implying that take-off could be an interesting design point for the propeller.[15].

2.4 Propfan

The propfan, sometimes called advanced turboprop or unducted fan is technology which has been tested since the 1970s, by NASA and other establishments. The concept has gained interest once again due to its potential to improve fuel efficiency, and thus reducing emissions compared to the traditional turbofan. The major difference between a propfan and a turbofan is that the propfan uses a propeller similar to the turboprop. Between the propfan and the turboprop the propfan has a higher Mach number in operating range, mainly because of the blade sweep used and typically generates thrust from the core as well as the propeller.

Most of the designs of propfans seem to originate from the NASA, in collaboration with Hamilton Standard, SR-1 through 7 series. This is a noteworthy research effort since they conducted wind tunnel testing of propellers at several different Mach numbers. The aim of the study was to evaluate the feasibility of propfan engines in commercial aviation. The propellers designed for higher Mach numbers, even the early SR-1 design achieves a propeller efficiency of 77 percent at Mach 0.8 [4].

One of the major challenges with propfan engines is the noise they generate leading to concerns in regards to airport regulations and passenger comfort. Another chal-

lenge can be the increase in vibration and structural loads on the airframe. It can also be challenging to handle the risks of a “blade out”, since there is no shroud to protect the cabin, wings and fuselage.

2.5 Differences Between Turbofan, Turboprop and Propfan

The main difference between the turbofan, turboprop and propfan engine thus boils down to operating conditions under which the engines are efficient. As discussed, the propfan aims to combine the advantages of the turboprop with the speed of the turbofan by using the high propulsive efficiency that can be achieved with a propeller for a higher span of Mach (see Figure 2.5). For this purpose the above mentioned technologies, such as swept propeller blades, need to be incorporated and control strategies developed.

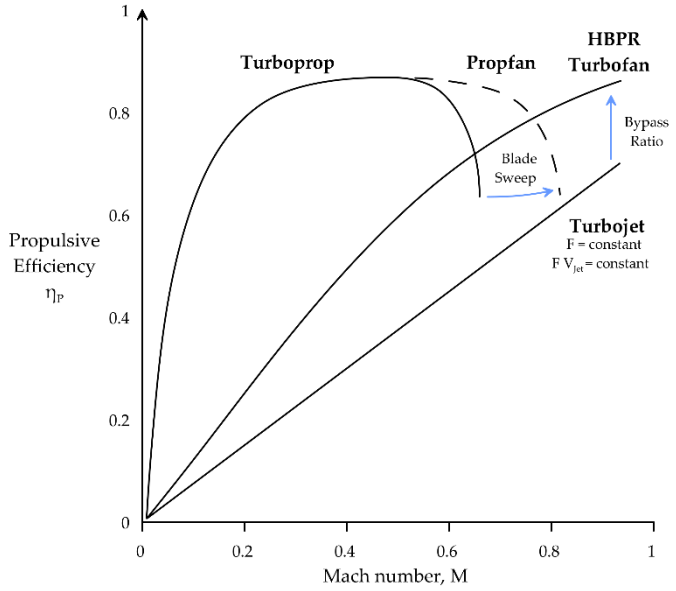

Figure 2.5: Propulsive efficiency for different engine types [16]

2.6 Mission Profile

A typical mission can be broken down into different segments of the flight. These are pre-flight, takeoff (TO), climb segments, cruise segments, descent segments, approach and landing. During these phases the aircraft systems and engines need to be operated in an optimized manner for a requirement of that specific segment.

Ground idle and flight idle are both defined as low as possible while still maintaining power, ability to reach full thrust quickly and services to the aircraft. Flight idle hydraulic and electric power as well as keeping the passenger air supply. But for both of these the lower the better, for the flight idle it means faster descent with-

out diving, and for ground idle it means less brake wear [17]. During the take-off sequence the engines are operated at maximum thrust to provide enough thrust for the aircraft to lift. This usually lasts for a few minutes. Take off is usually a point with the highest absolute temperatures and shaft speeds.

The next sequence is the climb phase, in which the aircraft climbs up to cruising altitude. The cruising altitude depends on the flight length, but is typically around 35000 ft or 10000 m. In this phase the engines are operated at maximum climb setting, which is a high thrust setting. At the end of this segment is the highest non-dimensional point of operations, "top of climb", which the engines often are designed for.

During cruise the aircraft flies at almost a constant speed and altitude. The aircraft then does a step climb and continues at a new cruise altitude relative to its decrease in weight as the engines consume the on board fuel, this is to optimize the fuel efficiency. The aircraft is operated at the cruise or at most max continuous setting. The max continuous is used in a one engine out operation to keep flying, and would likely result in a high acceleration if used during normal flight. The exact thrust generated depends on a number of factors, such as the weight, altitude airspeed and weather conditions.

When the aircraft reaches the end of cruise it begins the descent phase. During descent the aircraft descends down to approach altitude, in this phase the engines are operating at a reduced thrust to maintain a controlled descent. In the approach phase the aircraft prepares for landing and lines up with the runway. The engines are operated on flight idle thrust. In the event of a failed landing attempt the engines need to be ready for take-off-go around setting. Otherwise the plane can touch down and land. After the landing the engines are at ground idle to taxi to the gate.

2.7 Thrust Ratings

In aircraft propulsion systems the thrust rating is a crucial part, as it determines how much thrust an engine is producing at an operating condition. The rating selected can be influenced by a number of things, including flight altitude, flight Mach, ambient temperature, engine design, size and the environment in which the engine is operated. The thrust is typically measured in pounds force or Newtons.

Some ratings can be time limited in order to prevent the engines from taking damage, this typically applies to the take-off rating. The take-off rating is often limited to maximum 5 minutes and is used from the moment the aircraft accelerates from a standstill to end of runway at about 180 knots. The thrust ratings can be defined using the rating code and the definition in AS681 [18]. These can be seen in Table 2.1. Note that it is common for a civil engine to only use the "Nonaugmented" section of the table as they typically lack the afterburner required for augmented thrust. One exception to this was the famous supersonic passenger aircraft Concorde [19]

	Rating Code	Definition Military	Definition Commercial
	100.0	Maximum	Emergency
Augmented	90.0	Maximum Continuous	Maximum
	60.0	Minimum	Minimum
	55.0	---	Wet Takeoff
	51 to 59	Emergency or Contingency	---
		---	30-second OEI
		---	2-minute OEI
		---	2 1/2-minute OEI
		---	30-minute OEI
		---	Continuous OEI
	55.0	Maximum	
	50.0	Intermediate	(Dry) Takeoff
	45.0	Maximum Continuous	Maximum Continuous
Nonaugmented	40.0	---	Maximum Climb
	35.0	---	Maximum Cruise
	21.0	Flight Idle	Flight Idle
	20.0	Ground Idle	Ground Idle
Reverse	15.0	Idle	Idle
	5.0	Maximum	Maximum

OEI: One Engine Inoperative

Table 2.1: Power code table showing common thrust ratings for both civil and military engines

2.7.1 Thrust

Aircraft require different thrust from the engines depending on flight conditions, mission profile or even emergencies. The thrust may be different for altitudes and air speeds will vary greatly with changes in air density and the velocity of incoming air. The outside air temperature (OAT) will also affect the maximum thrust output and efficiency for the engine. Finally so called installation effects might effect the thrust, these include variables such as engine position and rotation but also effects on the incoming air that might be created by the aircraft's wings or fuselage.

During the design phase the thrust helps to determine the engine's capabilities and performance and is an important specification of any propulsion system. This also requires significant testing of a range of operating conditions to ensure the engine meet the desired performance and desired thrust.

2.8 Power Lever Angle

The power lever angle (PLA) is used by the pilot to choose a desired thrust ratings, thus determine the thrust generated from the engines. The PLA variables itself refers to what angle the power lever in the cockpit is positioned at. For some turboprops there is also a second lever that controls either the blade pitch directly or indirectly by changing the rpm limit for the propeller governor, in more modern turboprops this is sometimes controlled entirely digitally by the FADEC [17], [20].

2.9 Derating/FLEX

Derating of an engine refers to the engine operating at a lower power output than the maximum rated. There are several reasons to why an engine is run at a derated state, these include extending the lifespan, with reduced wear and tear on components or reduced fuel consumption. It can also increase the reliability of the engine. The harsh conditions of an aero engine are lessened when an engine runs at a derated state due to the component temperatures being lower which leads to a longer component lifespans. Derating in an aero engine reduces the thrust and performance of the engine. For some engine manufacturers the derates goes in steps of 4% up to 24% derated thrust wise [21]. A derated engine cannot run at its full TOGA thrust capacity during the take-off but is instead limited to the thrust settings given by the derating.

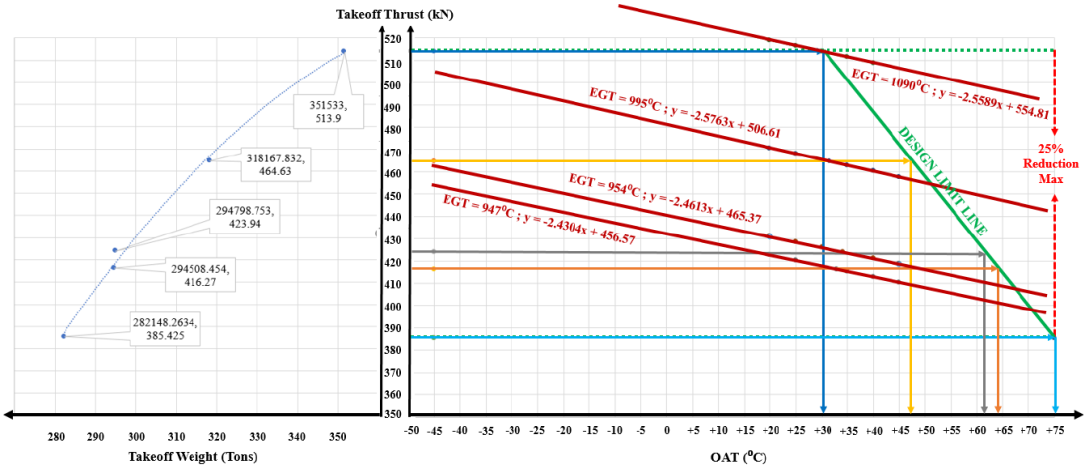

Figure 2.6: An example of assumed temperature [22]

Flex is when the engines are reduced in thrust output to meet new operational requirements. This is done by setting a new outside air temperature (OAT) higher than it actually is, and thus tricking the flight computer to lower the thrust available not to damage the components. An example of an assumed temperature can be seen in Figure 2.6. Flex only works when the thrust is already maximum, otherwise it

the engine will spool up N1 instead of reducing fuel to meet the new OAT. The new performance is calculated by the flight computer and TOGA can be recovered at any moment. The thrust settings parameters are not considered as take off limits.

2.10 Measurement of Efficiency

To easily be able to check how the engine compares with similar turbofans, the measurement of efficiency chosen was $\eta_{overall}$. This efficiency is calculated by dividing the propulsive power by the fuel flow energy [23].

$$\eta_{overall} = \frac{F_n \cdot v_{inf}}{FuelEnergy} \tag{2.10}$$

The overall efficiency will be a product of the propulsive efficiency and the thermal efficiency. In this case the propulsive efficiency will consist of both efficiencies from the nozzle, propeller and stator, contrary to a turbofan in which case it is just nozzles and no propeller. The propulsive efficiency for a nozzle can be calculated from the exit speed compared to the ambient speed of a nozzle. These differences make it harder to compare between the engine types, especially considering the multiple nozzles and propulsive efficiencies needing to be calculated.

$$\eta_P = 2 \cdot v_{inf} \frac{\dot{m}_{exh} \cdot v_{exh} - \dot{m} \cdot v_{inf}}{\dot{m}_{exh} \cdot v_{exh}^2 - \dot{m} \cdot v_{inf}^2} \tag{2.11}$$

2.11 Compressor

The compressor operates by being driven by a shaft converting work or applied torque to a compressed fluid. It is composed of alternating rows of static and rotating blades, known as stators and rotors. Compressors with multiple rows of blades are referred to as multistage compressors, which are commonly used in modern aero engines [24].

Despite its importance, compressors can experience two major issues: stall and surge. Stall occurs when the flow becomes separated from the blade or vanes, which can cause significant loss of pressure and power output. This can lead to a variety of issues, such as vibrations, decreased performances, and in some cases damage to the compressor.

The other major issue that can occur in compressors is surge, surge can be seen

as a more severe form of stall. It is caused by a sudden change in flow rate or pressure that disrupts the flow through the compressor. This sudden loss of pressure or flow, can cause loss of power and significant damage to the engine if left unchecked. Surge can occur due to a variety of factors, including sudden changes in atmospheric conditions, changes in throttle settings or load, or even worse, mechanical failures within the compressor itself [25].

In the design of aero engine, compressors are scaled to meet the requirements of specific operating conditions. One way to adjust the size of a compressor in the early stages of design is to use a scaling approach based on non-dimensional properties. This involves using the specific speed of the compressor to determine the scaling factors which are then used to achieve a desired performance characteristics at the design point.

The component maps used in this project are part of the GasTurb standard library and include maps for the LPC, IPC, HPC, HPT and LPT. Although these are good approximations the performance map for the LPC assumes a low hub to tip ratio, which could be argued to not hold true for this model in particular.

2.11.1 Operability of the Compressor

The compressor performance depends on a specific bleed flow and stator vane settings, these would be in front of each compressor stage as inlet guide vanes to guide the flow into the compressor. In this project the operability was only managed using bleed settings and no variable stator vanes in the compressors. This could lead to a penalty in specific fuel consumption due to bleed work being a form of lost power or thrust. The performance map can also be altered by the bleed location, bleed flow rate and the stator vane orientation, and not only by the fixed geometry. To be able to capture all of the impacts the model would need an individual compressor map depending on both bleed, and stator vanes settings. The performance and operability will be different with a different set of speed lines for the same operating state. According to Brooks it is impractical to have different maps for different bleed rates and positions within a compressor and thus this thesis did not use more than one map per component.[26].

2.12 Turbine

The turbine works by extracting energy from high energy air to generate torque on a shaft and in turn the compressor [27]. All gas turbine engines, turbofans, turboprops etc. have a turbine downstream of the primary burner. The power is obtained by expansion of fluids, this power can then be used to drive either a compressor or customer power output, such as a propeller or auxiliaries.

The compressed and burned fuel and air mix leaving the combustor can be as hot as

1600 ℃ and flows directly into the first turbine stage of which the rotor and stator blades might have a melting point of 1250 ℃ [28]. This is a significant problem for engine durability. A common solution used in all modern gas turbines is to cool the blades with relatively cold air from the compressor that has not gone through the combustor. The air then runs through the blades and out into the flow, thus cooling the surface of the blades.

Some engines use a free power turbine, which is not connected to any compressor and such can spin independently to the other shaft [29]. The free power turbine can be used to drive any desired power load such as propellers or helicopter rotors, as it can give a higher torque and a lower rotational speed. A free power turbine also causes more complexity to the system, since the characteristics and power curve are determined of the flow coming into it [30].

3
Method

The following chapter will outline the main approach to achieving the desired goals. It will also outline the tools used in the project. Note that the generally desired performance, target and/or outcome during the following steps was to provide methods that result in high propulsive efficiency together with high operability throughout the flight envelope.

3.1 Tools

The following section outlines the tools that were used during the thesis and aims to give the reader a fundamental understanding of how these work.

3.1.1 NPSS

A cornerstone of the work was to learn and use the already mentioned software package developed by NASA, SwRI and WV called Numerical Propulsion System Simulation (from now on referred to as NPSS). This software package enables the user to assemble and simulate all the components critical to the thermo and fluid dynamic performance of a 0D simulation, with low-level access to the code of most components. The language used for this bases its syntax upon C++ and allows for object-oriented programming (OOP) while, contrary to C++, being dynamically typed and not requiring any (while still allowing one to do so!) compilation before execution. The most critical concepts on which NPSS is based are the use of so-called elements, flow stations and links. Once these are established the model is solved according to either automatically generated or user-specified constraints, dependent and independent variables.

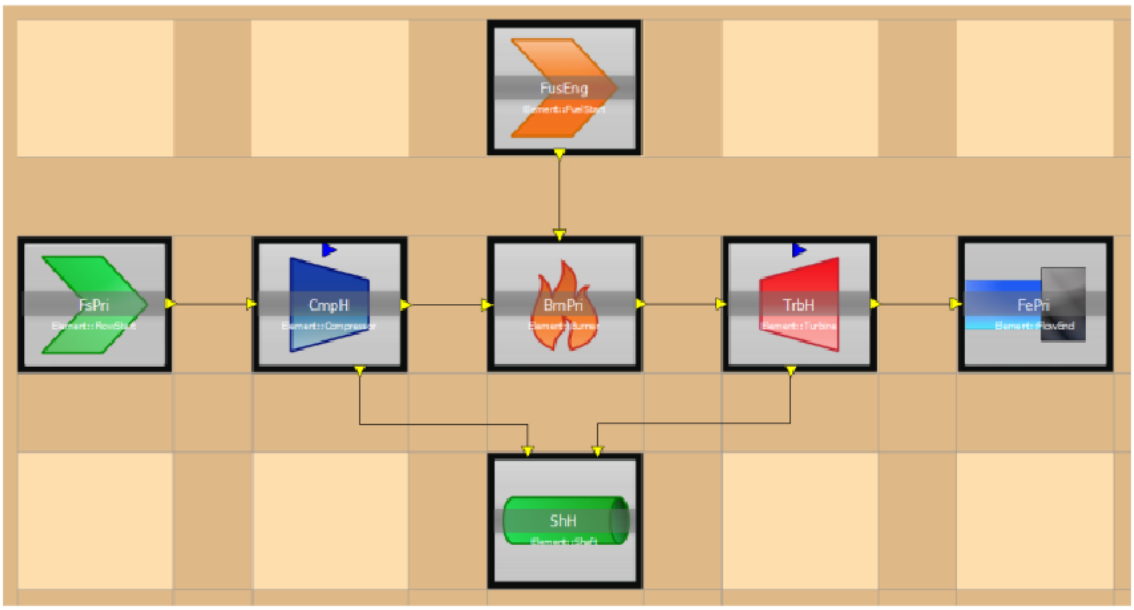

Figure 3.1: Example of a simple Brayton cycle in NPSS made up of (going left to right) a flow start, compressor, burner, fuel start, shaft, turbine and flow end element. Note the black lines with yellow arrows that represent the links between elements.

3.1.1.1 Elements

Elements are the building blocks of NPSS and, as encouraged by SwRI, one can often think of them as LEGO pieces that can together be used to build more complex structures. SwRI and WV recommend in their training material that one should take the approach of breaking down existing cycles/engine configurations into smaller pieces in order to get a general understanding of which elements are required in order to construct a representative model in NPSS. One example of this would be to break down a simple Brayton cycle engine into a compressor, burner and turbine elements with a shaft element that connects the compressor and turbine (see Figure 3.1). It is important to keep in mind that while NPSS is primarily designed to model propulsion systems, it is in no way limited to this and the user is free to write their own elements with either existing properties or even entirely new ones. As such there are elements relevant to everything from electrical systems to plasma and nuclear research but a major part of developing a new engine concept might still be to write a custom element that is better suited to model the wanted effects [31]. Each element then has its own requirements in terms of ports and so-called “sockets”.

Subelements are a different class compared to elements, they work the same. The difference lies in where the element is executed as the subelement exists within an element instead of the engine model. The subelement thus cannot work on its own, but requires calls from the element in order to funciton properly. Each subelement plugs in to a socket of an element fulfilling a certain function, some sockets are required to have subelements in order for the element to function.

3.1.1.2 Links

Links in this case represent the ducting or piping in-between turbines and nozzles or the fuel pump and burner, etc. . The model requires each link to have a specified start and end point. Usually these points are reserved to only allow one connection but others such as the connections on the engine shafts allow for multiple connections.
The links between each element's different ports follow some basic rules in NPSS. Each output port has to be connected to an input port of the same type. As such a fuel port outlet from for example a fuel start element has to be connected to a fuel port inlet on a burner element. The burner element in turn could have both a fuel and flow input port in order to compute temperature rise, air-fuel ratio, etc. which in turn get sent out through a single flow output port (see Figure 3.1).

3.1.1.3 Flow Stations and NPSS Solver

NPSS implements a 0D approach in order to solve the given model. The solver is built on the newton Raphson method, which can cause instabilities with local high and low maximum/minimum. In this process, each flow station is computed from the previous element and passed along to the next according to the specified links. The specified independent variables are then varied by the solver until the model satisfies the set constraints and equations for dependent variables. Which dependents and independents are enabled can vary between design and off design.

The flow station's properties are dependent upon the selected thermodynamics package but generally hold properties such as static and total pressure (ps, pt), enthalpy (h), area (A), mass flow (W), etc.
There are also a number of solver settings that can be changed or tweaked, but the ones changed during this thesis were; max number of iteration, max number of Jacobians, default tolerance and default perturbation.
Convergence and convergence ratio is important when checking the results from a run, if the solver has not converged at all, the solution becomes invalid. The convergence ratio can be used to describe how well a model or solution has converged. A convergence ratio above one indicates a diverged solution, and a lower value indicates a faster convergence.

3.1.2 Visual Studio Code

As a simplified version of Microsoft's primary development tool, Visual Studio, Visual Studio Code gives an easy-to-use code environment with support for many different languages. By using the C++ syntax highlighting preset one can work with NPSS code in a more user-friendly way, although it should be noted that some quality-of-life features that are commonly associated with a modern C++ IDE are lacking because of the subtle differences between C++ and NPSS. Examples of these missing features are auto-completion, code suggestions or any form of IntelliSense or similar AI accelerated code tools.

3.1.3 Git and Azure

In order for teams or even a single person to work efficiently with larger code bases, so-called version control systems are used. These keep track of changes and enable the branching of projects in order to develop features on their own before later merging these changes back into the main branch. Azure and Git were used during this project.

3.1.4 Optoprop

The Optoprop code, written in python by Alexandre Capitao Patrao at Chalmers University of Technology, allows the user to generate propeller geometries and performance estimations given a set of desired parameters such as advance ratio, blade count, rotor diameter, hub-to-tip ratio, etc. Once the geometry has been generated for a given design point the code can be switched over to off-design analysis which allows the user to investigate the performance of the propeller for different conditions. A further mode in the code allows the user to not only evaluate off-design performance but to sweep through a set of advance ratios in order to establish performance maps. It must be noted here that a similar use case of Optoprop has been shown before to compare the performance of Boxprops by Patrao A. C. [32] for the python version and by Isak Johnsson [11] for a previous version written in Matlab. However, two counter-rotating rotors were investigated in those works instead of the single rotor investigated in this project.

3.2 Extending Optoprop to Include Blade Sweep

In order to accurately approximate the propeller efficiency of a high speed propeller, blade sweep has to be accounted and designed for. Without blade sweep the tips or even a large portion of a propeller will quickly reach supersonic speeds at which point the efficiency can drop significantly.

The lack of blade sweep in Optoprop was seen as one of the most critical issues when initially comparing computed propeller maps with existing ones from Hamilton Standard. Because of this, a simple implementation of blade sweep was added to the Optoprop design and analysis code. Assuming that by changing the coordinate system to be cylindrical, the blade sweep of a propeller follows the same principles as wing sweep does for an aircraft. Thus if one wants to keep their relative Mach number below a certain threshold the, rewriting of 3.2 gives:

$$U_{tip} = \omega \cdot r \tag{3.1}$$

$$M_{rel} = \sqrt{(U_{tip} \cdot a)^2 + M_0^2} \tag{3.2}$$

$$\beta = cos^{-1} \frac{M_{rel,target}}{M_{rel}} \tag{3.3}$$

Assuming each blade section to be of equal size the total offset from the geometric mid line then becomes the sum of all previous elements offset relative to the previous. This can be computed with the tangent of the element sweep angle and the element radial length.

$$x_{rel,offset} = tan(\beta \cdot (r_i.r_{i-1})) \tag{3.4}$$

$$x_i = \sum_{n=0}^{i} x_{rel,offset}(n) \tag{3.5}$$

Note however that very few propellers are made up of sections with equal chord and as such the delta in chord has to be taken into account for each blade element and the resulting leading edge sweep angle thus is a combination of chord delta and mid line sweep angle.

3.3 Propfan Performance Map Element

A key part of running the propfan model was to estimate the fan performance depending on blade pitch and advance ratio. This required modifications to the propeller element in NPSS that would allow for use with results from Optoprop. The following changes were made to the Propeller element; made it so that the diameter can be set and the disc loading is calculated instead of the other way around. This makes it possible to change the diameter easily for the design point. This also required changes in the PropCT subelement, which contains the performance map of the propeller data.
The lookup-table design order was modified to better suit the needs of the propeller data. The previous model only used two variables to get the CT, the new table was sorted to interpolate the CT value based on Mach number, advance ratio, and CP. The efficiency of the propeller was then calculated from these three according to equation 2.6.
Another table with 100% of the swirl losses recovered was also added and a variable for interpolating between 100% and 0% was introduced.

The next step was to write code that formats results from Optoprop or NASA data into a performance map readable by NPSS and then plug this map into the propeller map socket of the propeller element. The previously mentioned interpolation swirl loss recovery variable was assumed to be 60% For this project. The 60% were chosen based upon research by Miller [13] showing a possible recovery of 40% swirl losses in 1988 and Larsson [2] assuming 90% recovery in their work in 2013. Thus 60%, a 50% increase from 1988 but reasonably lower than the stated 90% by Larsson, could arguably be seen as a possibility for an engine introduced in the next few decades.[10].

Finally, a switch parameter was introduced in order to easily change which propeller data would be used in the simulations. The model can be set to use either NASA, Optoprop, or a mixed map for propeller performance. While there are three options these are only two different sets of propeller data. The NASA option uses digitalized data from a Hamilton Standard study of 1978, whereas the Optoprop data was simulated data from the Optoprop code as described earlier. The mixed result uses the experimental NASA data where it is available but then extends this with the simulated results to reach higher advance ratio regions. This resulted in an accurate performance map for the region with lower advance ratios while still allowing the model to compute an approximate result for higher advance ratios. The breakpoints for which this occurs can be seen in Table 3.1. The breakpoint can also be seen in the contour plot presented in the results for the mission profile (see Figure 4.5). This propeller data allowed for a full mission sweep without any extrapolation in the performance map.

Table 3.1: Breakpoint for data in mixed propellermap

Mach Number	NASA	Optoprop
<0.55	J <3.50	J >= 3.50
<0.60	J <4.00	J >= 4.00
<0.80	J <4.25	J >= 4.25

3.4 Development of Thrust Ratings

By selecting thrust rating, the pilot essentially describes how much of the available thrust they want to use at a given condition. Thus, in order for a thrust rating to be established the maximum available thrust has to be computed first.

Because of time constraints, this thesis had to limit the number of ratings that were investigated to only a single one, and since the take-off rating is one of the most important ratings it was the rating that was focused on. Since the take-off rating is the highest commonly encountered rating the model would have to be run to the maximum possible thrust at a number of conditions including, TOC and TOEoR but also some Mach and altitude conditions between these. This was done by sweeping through increasing values of fuel mass flow until either a constraint was reached or the model would stop converging.

3.5 Model

The NPSS model was modeled closely to a conventional turbofan engine with a propfan added instead of the regular ducted fan. The overall layout of the core includes an LPC, IPC, HPC, HPT, and finally LPT (see Figure 3.2). The HPC and

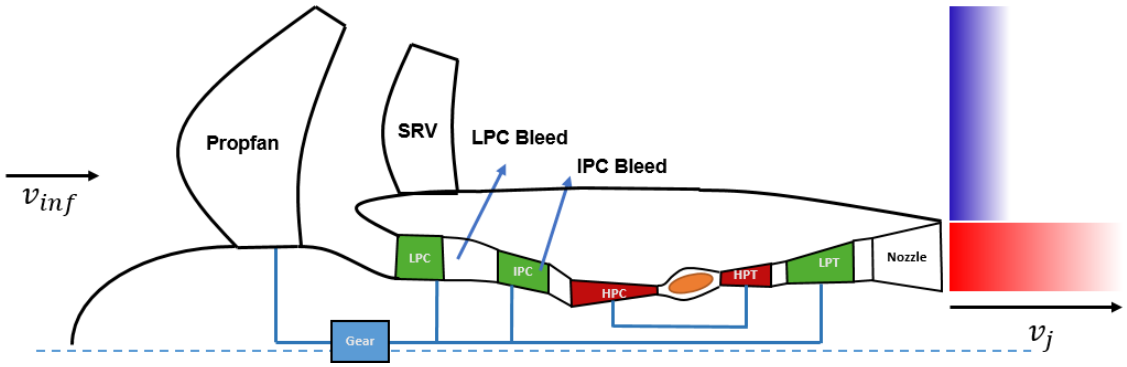

Figure 3.2: Schematic illustration of the component layout in the NPSS model

HPT are coupled with a common shaft as are the remaining LPC, IPC, LPT as well as the propfan in front of the core. Between this low-power shaft and the propfan itself, a gearbox was added in order to gear down the shaft speed from typical LPC, and IPC speeds to the much lower shaft speed typical for propfans/propellers. The gear ratio was determined from the design point but ends up similar to the gear ratios found in common turboprop engines, around 8.5:1. All of these components are modeled as elements in the NPSS model.

One simplification made in the model was that the pressure increase behind the propfan was not taken into account for the LPC. In reality, one could expect this to have an impact on the LPC performance although the proximity to the hub would suggest that the impact would be small given that the flow acceleration and pressure increase around the hub of a propeller usually is quite small. Further, this also implies that the air that would have been inhaled by the LPC was included in the propfan thrust calculation even though in practice the flow would be obstructed or at least affected by the LPC inlet in this region. Once again, the impact of this was expected to be small on the overall engine performance. The naming of the flow stations follows the SAE standard for aero engines with a few noteworthy stations being F041 (directly after the first row of stators in the HPT) and F080 (nozzle exit).

3.5.1 Mission Profile

The mission profile was used to define both design and off-design points for the NPSS model and the deciding factors for choosing a mission profile were the accuracy of the data as well as the level of detail. These were a result of the aim of simulating an entire mission profile and thus including details like step climbs and different climb segments was seen as an advantage.

3.5.2 Design Point

The existing model in NPSS was designed at top of climb. This is most often the aerodynamically hardest point to achieve sufficient thrust at for a turbofan, hence

why this was chosen as a designpoint. Top of climb conditions in this case include a thrust of 31.9 kN, Mach 0.78 and a OAT of ISA +15 dK. The original model had a set efficiency of 88% for propeller thrust, the updated propeller data from NASA gave a calculated propeller efficiency of 84%.

3.5.3 Off Design

In this model, the stator vanes are not modeled as variable except for the propfan stator, which is modeled by the swirl loss recovery method descibed above. The model was run both with and without temperature and shaft speed constraints. These constraints were set to values similar to those used in similarly sized and performing engines. These in combination with a stall margin based on the design point stall margin are deemed to give reasonably close results to an actual engine. Examples of the points ran can be seen in Table 4.1.

3.5.4 Solver Settings and Constraints

All of the following off-design points were run with the following, see Table 3.2, set of independent, dependent variables and constraints. Note that the initialisation points, used to improve solver convergence, were set to solve towards a set total net thrust ($Perf.FnTot$) whereas the following throttle sweep points solved towards a set fuel mass flow (BrnPri.Wfuel).

Table 3.2: Solver independents, dependents and constraints

** Solver Mode **	** Solver Constraints **
switchDes = OFFDESIGN Pset.switchParm = THRUST or Pset.switchParm = WFUEL	Pset.dep_T41 = 1850 K Pset.dep_T3 = 975 K Pset.dep_NcPctHP = 103% Pset.dep_NcPctIP = 103% Pset.dep_NcPctLP = 103% Pset.dep_NcPctLT = 103% Pset.dep_NLP = NLPdes · 105% Pset.dep_NHP = NHPdes · 105%
** Solver Dependent Variables **	** Solver Independent Variables **
dep_PropFan_pwrRatio	ind_PropFan_pwr
dep_CmpI_SMN	ind_CmpI_Bleed
dep_CmpL_SMN	ind_CmpL_Bleed
Pset.dep_Power	Pset.ind_Wfuel
CmpL.S_map.dep_errWc	CmpL.S_map.ind_RlineMap
CmpI.S_map.dep_errWc	CmpI.S_map.ind_RlineMap
CmpH.S_map.dep_errWc	CmpH.S_map.ind_RlineMap
TrbH.S_map.dep_errWp	TrbH.S_map.ind_PRbase
TrbL.S_map.dep_errWp	TrbL.S_map.ind_PRbase
NozPri.dep_Area	InletStart.ind_Wc
ShH.integrate_Nmech	ShH.ind_Nmech
ShLGEAR.integ_shaftTheta	ShLGEAR.ind_theta
ShLTURB.integrate_Nmech	ShLTURB.ind_Nmech
ShLPROP.integrate_Nmech	ShLPROP.ind_Nmech

3.5.5 Constrains, Independents and Dependents

The model was run under some general component constraints for off design. These were both temperature based and rotational speed based constraints. For the flow station F41, after the HPT stator and before the HPT rotor, the maximum allowed temperature was set to 1850K, for flow station T3, directly after the HPC, the maximum was set to 975K. The shaft speeds were set to a maximum of 103% of design point corrected speed and 105% of design point absolute shaft speed for each shaft.

In addition to these, some new independents and dependents were introduced for off design cases. These were created in order to keep the equations balanced when switching the model from targeting a set thrust, to instead target a set fuel mass flow. As such there always exists a pairing of an independent controlling fuel mass flow and a dependent on either fuel mass flow or thrust acting as a target value. When the model was set to adjust for thrust the pairs used are; IPC Stall margin and bleed, stall margin for LPC and bleed, propeller power ratio and propeller power, set net total thrust and fuel mass flow, followed by a number of independent

/ dependent pairs created automatically by the NPSS elements (see Table 3.2.

3.5.6 Solver Instability

During the thesis some instabilities were noticed in the Newton Raphson solver that NPSS uses, these could be solved or worked around but often lead to confusion and made the model feel "fragile". The instabilities were usually encountered when the off design point changes were too harsh, i.e. when changing from TOC to TO. The solution to this was to just run the second point two extra times, one to get convergence, and one to verify that the results would not drift after convergence. Some solver settings were also modified, the default perturbation, which had some impact on achieving convergence, but the solver seemed to always have some outlier case where it either overshoots or underestimates the results but still reports the cases as converged.

The off design points ram using either thrust ratio or power ratio to control the propfan thrust. For some configurations the thrust ratio approach to controlling the propfan had worse convergence, likely due to component efficiencies being taken into account leading to the thrust ratio being coupled to multiple other variables. The power ratio approach solved this since it could be directly calculated from the LPT power output for each iteration.

3.6 Analyse the Finalised Model Throughout a Complete Flight Mission

Investigating a singular off-design point or even multiple, in regards of engine performance, can be useful but it did not generate much information on where in the engines throttle regime the engine was operating. In order to determine this, the ambient conditions needed to be kept constant while sweeping the engine throttle. Since the throttle scheduling strategy was not fully developed at this point, a certain amount of educated guesses as well as trial and error were required in order to find engine parameters that predictably vary the engines thrust output. Note that while this might have been functionally very close to the control that the power lever provides the pilot, they are in fact different in that the PLA is expected to result in a linear variation in throttle for a given change in PLA. The direct control over engine parameters however, usually results in non-linear behaviour that is later on compensated for in the final scheduling tables.
During the above outlined process, various bleed valves and scheduling for these had to be implemented. Using a tool like NPSS was of great advantage for this since the mass flow through each bleed valve could be allowed to vary as seen fit by the solver in order to fulfil a given requirement such as a specific stall margin on a relevant compressor.
Once all of the above were completed the model could have used as an element in a more general flight mission model which would include multiple mission segments such as take-off, climb, cruise, descent, landing, etc. This would allow for a solid

verification of the operability given the developed control schedules and thrust ratings. During these tests there are some key factors to check, these are operability in component maps and keeping enough stall margin. These two are quite closely related, since good operability requires a good stall margin. However due to time constraints the engine was never combined with an airframe model and thus was only simulated on its own.

3.6.1 Off Design Points

The off design poins were analaysed as steady state points, not as transient. Each point represent a typical point in a mission profile. These were created from a known thrust requirement and flight conditions.

3.7 Post Processing of NPSS Results

In order to better understand and visualise the simulation results from NPSS, compressor and turbine maps were plotted with each operation point marked in the maps. This gave a quick overview of the feasibility of operating the engine at each point and also indicated whether or not additional bleed might be required in order to uphold sufficient stall margin. A plotting tool was available at GKN and while this solution was versatile and enabled the user to plot a variety of parameters, it did not allow the user to only run a single point. Instead a sweep over one or two parameters was required. Due to the nature of how the solution was written each simulation point would take substantial time to run and save all the data. This meant that in order to analyse broader sets of points, as would be required when simulating a complete engine scheduling envelope, a faster solution would be required. Thus, a python module was written that was capable of importing NPSS simulation data in the format of a so called “ColumnViewer” as well as translating any component characteristics map written for NPSS into graphs and scale these according to the simulation data. This gives the user the possibility of plotting any amount of points without any performance overhead for the NPSS simulation itself.

What can be noted however, is that the contour graphs do not reflect efficiency losses calculated from tabulated Reynolds compensation data. These losses are not captured in the performance map data that the python code uses. The line and point graphs presented do capture these losses since they use the calculated performance by NPSS.

4
Results

This chapter will outline the results of the project. This includes necessary changes, mission profile and results from different configurations and simulations

4.1 Mission Profile Choice

The chosen mission profile was provided by C. Xisto at Chalmers University of Technology and was generated using Pacelab. This data enabled a direct comparison in SFC and performance throughout the entire flight envelope which was deemed to be more important than representing a feasible platform for a first implementation of a propfan engine. If the latter would have been of interest, a mission profile for an A319 or A320 could have been more fitting.

It is worth noting that one alteration had to be made to the chosen mission profile since the original data contained negative thrust values for parts of the descent segment. While it is very likely that this is correct and simply caused by the ram drag of the engine exceeding the gross thrust, getting NPSS to converge proved very difficult for these points since the model was not built to handle negative thrust requests. Because of this, all points were limited to a minimum thrust of 1kN throughout the entire mission profile.

For the propfan engine, the two most challenging conditions were identified to be TOEeR and TOC. TOC as it was the most non-dimensionally challenging condition for the engine's core and TOEeR as it signified the point of highest thrust from the propfan itself.

Table 4.1: Mission profile points

Operation Point	Time [min]	Altitude [ft]	Mach	Thrust [N]
TO	0.3551	0	0.2438	123664
IC	2.671	5000	0.4129	73035
TOC	20.33	35000	0.78	31873
CRZ	26.49	35000	0.78	23780

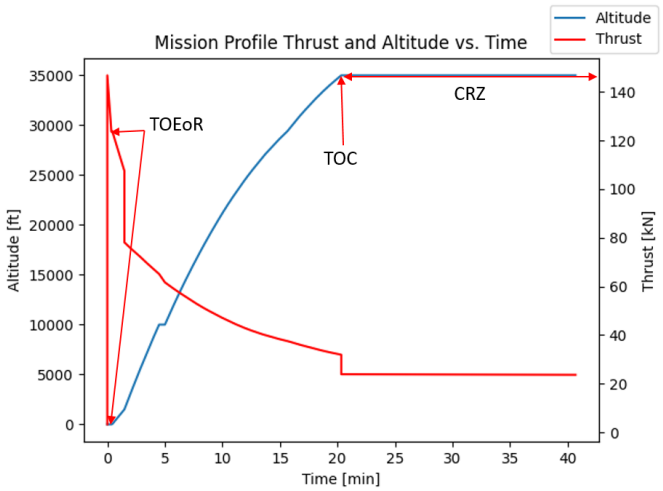

Figure 4.1: Mission profile for the A321 used with points marked. Limited to take-off, climb and initial cruise.

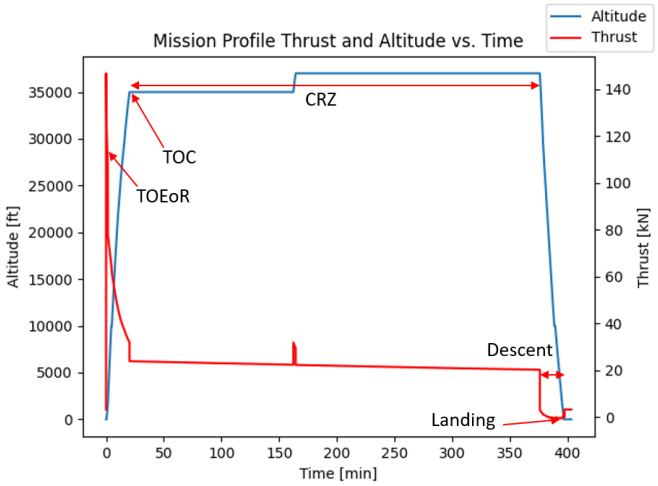

Figure 4.2: Mission profile for the A321 used with points marked. Whole mission overview

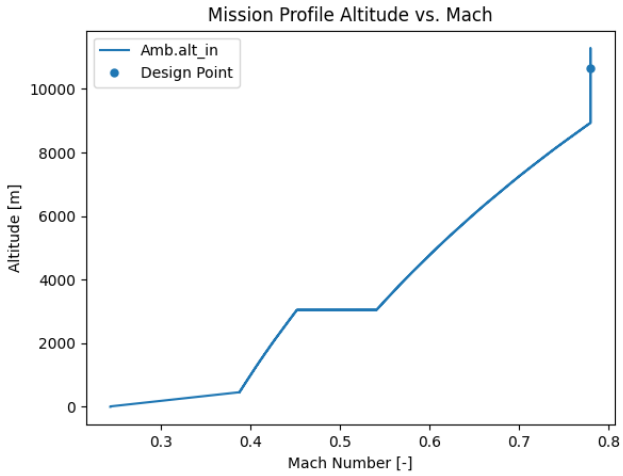

Figure 4.3: Mission profile shown as altitude, Mach number

Figure 4.3 shows full profile, and thus the climb profile in terms of altitude and Mach number.

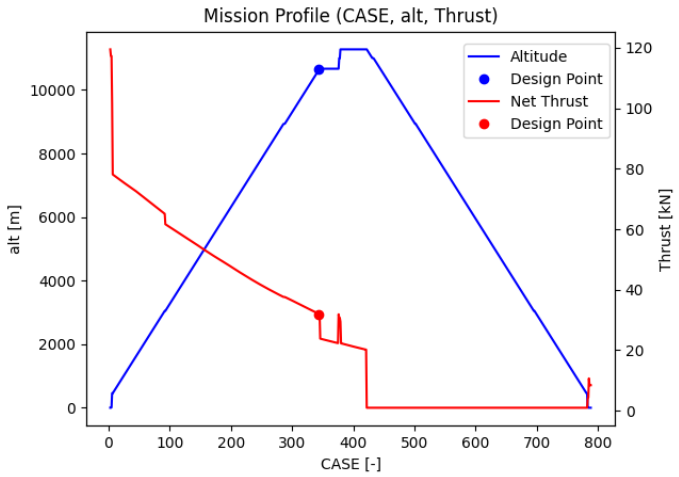

Figure 4.4: Mission profile vs case, showing alt and thrust for a single engine

The figure shows the thrust and altitude as a function of simulation case number. This resulting profile follows the predefined input of the A321 flight envelope.

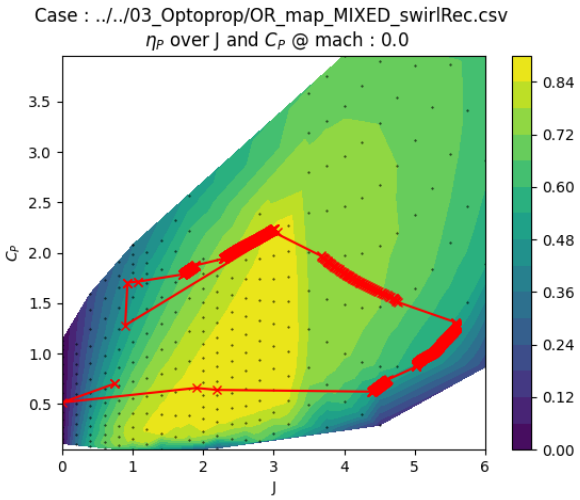

Figure 4.5: shows the mission profile in a mixed (NASA for J <3.5 and Optoprop for J >3.5) propeller map

In Figure 4.5 we see that for the extended data set of the propeller performance the whole mission profile is well within the limits of the propeller. The higher part of advance ratio is from Optoprop while lower is the experimental NASA. Here it can be seen that the Optoprop simulation is a good contribution and extension to the dataset. Note that while the contour is plotted for $MN = 0$, the mission profile does of course include other Mach numbers which correspond to other data tables in NPSS.

4.2 Power Ratio

In order to control the distribution of work done by the propfan relative to the core a metric from now on referred to as the power ratio was introduced. It describes the fraction of power from the LPT that is sent to the propfan instead of going to the LPC and IPC. In a practical implementation, this could be achieved by controlling the propfan blade pitch while monitoring a torque sensor, as is done in some turboprop/turboshaft engines [33]. Initially a ratio in thrust between propfan and core was also considered but this lead to multiple possible solutions due to variations in efficiency and problems with operability at low throttle. The power ratio approach does not exhibit these problems and always gives a single solution for any condition due to the calculation only taking the current power into account without any downstream losses due to efficiency.

A sweep over a range of power ratios was then performed in order to find suitable values. This was done for the design point conditions.

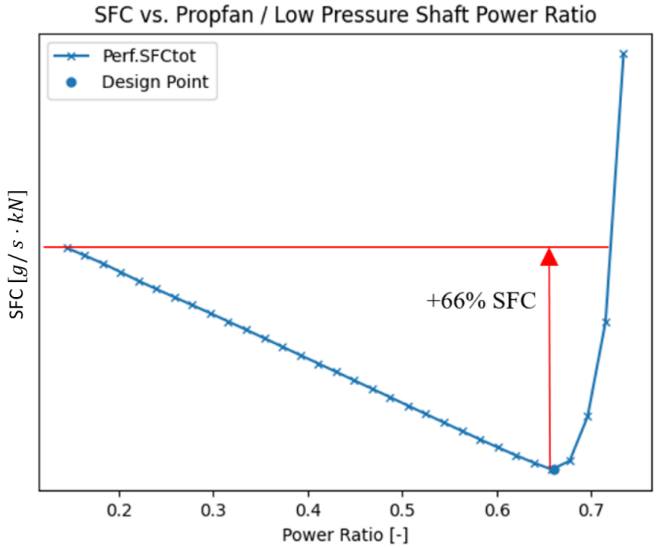

Figure 4.6: SFC for a sweep of power ratio

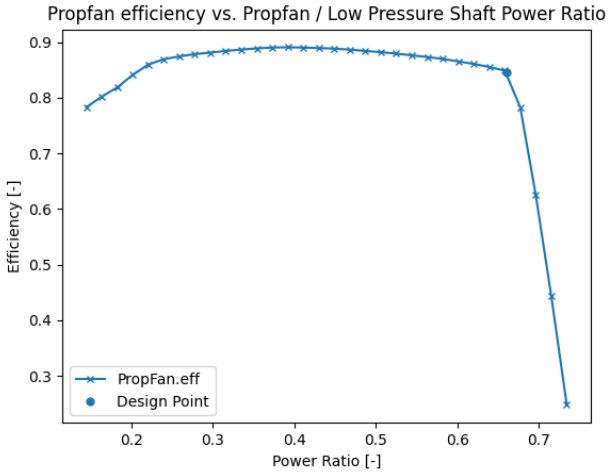

Figure 4.7: Propfan efficiency for a sweep over of power ratio

Looking at the results from this a clear minimum point can be seen at a power ratio of 0.66 (see Figure 4.6). The sharp increase in SFC following the minimum point coincides with a rapid decrease in propfan efficiency. Considering the linear decline of SFC between power ratios of 0.2 – 0.66 despite the propfan efficiency staying almost constant could suggest that a propeller design that is more optimised for higher thrust could lead to even higher power ratios being more optimal.

An analysis of how the cruise performance would be effected by choosing this power ratio was conducted following the design point analysis.

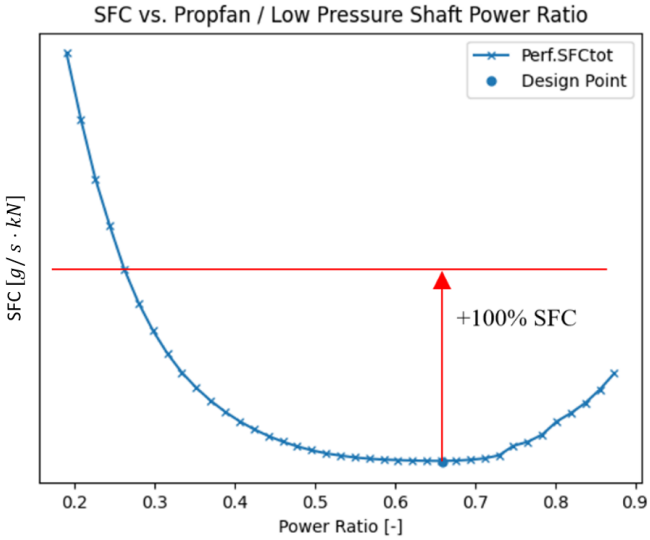

Figure 4.8: SFC during cruise conditions for a sweep of power ratio

Sweeping through a range of power ratios at these conditions shows that no further improvement to the SFC can be gained from simply changing to a different power ratio. It is worth noting however, that the increase in SFC before and after the minimum point behave in a different manner compared to the design point (see Figure 4.8). Further, the propfan efficiency ends up being higher for a large span of different power ratios compared to the design point (see Figure 4.9). This effect is likely due to the lower thrust requirement leading to lower blade loading and the propeller thus ending up with a higher efficiency according to the propeller map.

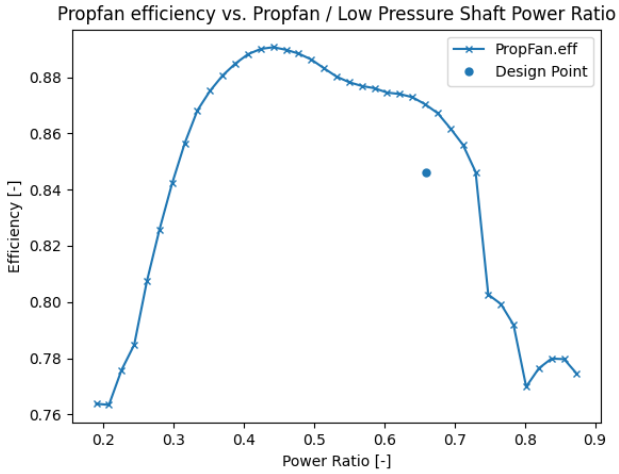

Figure 4.9: Propfan efficiency at cruise conditions for a sweep of power ratio

One might expect this increase in propeller efficiency to lead to a lower SFC (as would be expected from a typical turbofan engine) but this is not the case for the propfan engine. In order to understand the reason for this, one will have to consider operability and the previously mentioned added bleed ports.

4.3 Operability and Bleed

The following will present the results from a number of different off design simulation covering the propfan engines behavior when decreasing throttle from the mission profile typical throttle. These simulations were run with a targeted fuel mass flow instead of thrust but followed the same requirements in terms of stall margin and spool speed constraints.

4.3.1 TOC

When transitioning from TOC to cruise conditions the aircrafts thrust requirement decreases significantly (see Figure 4.4). The change in thrust leads to a decrease in mass flow which effects the corrected spool speed for the engine components. In order to keep operability the propfan engine has two bleed ports (one from the LPC and one from the IPC) which help with regulating the pressure ratio and thus keeping the compressors below the stall line at the cost of engine efficiency. The fraction of mass flow that has to be bled in order to keep operability increases as the engine is throttled back (see Figure 4.10) and during cruise the engine can be expected to bleed 6-7% from the IPC and LPC respectively. Taking a closer look at how this impacts the SFC (see Figure 4.11) shows us that the propfan engine has a 1.5% higher SFC during cruise than at TOC. Noteworthy is the slight decrease in SFC ahead of the increase towards cruise throttle, which might implicate that there is some potential for optimization that could net a lower SFC at cruise if one would accept a higher SFC at TOC.

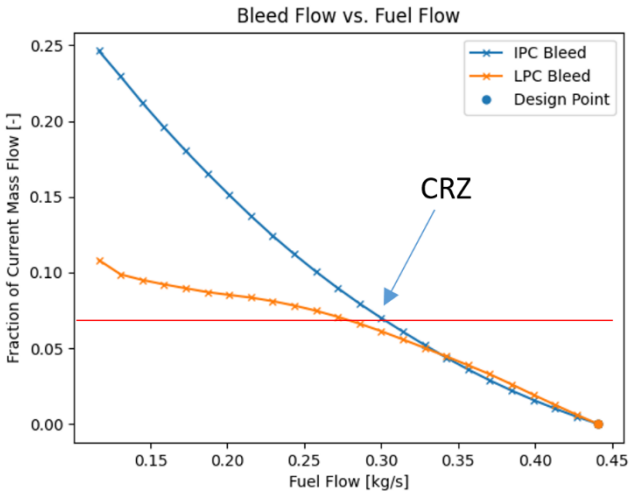

Figure 4.10: Bleed flow fraction at TOC conditions for sweep of fuel flow

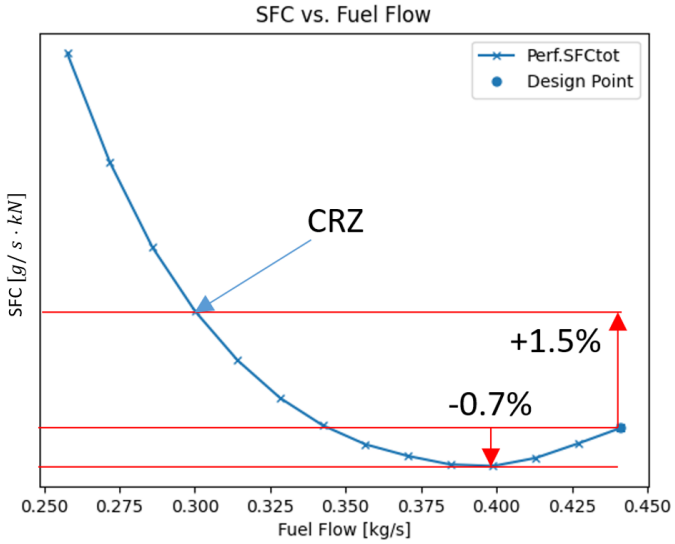

Figure 4.11: SFC at TOC conditions for sweep of fuel flow

Looking at the propfan efficiencies over a range of fuel flows shows a continuation of the behaviour that could be seen between TOC and cruise conditions. Instead of looking at propfan efficiency for different power ratios we now see that the propfan efficiency increases as the engine is throttled down (see Figure 4.12). This drop in efficiency occurs as the propfan leaves the area of reliable NASA data and instead enters the area in which simulated Optoprop data is used (see Figure 4.13). Note that the total thrust at these throttle ranges is less than 15kN (less than half of TOC) and that the thrust produced by the core almost reaches zero for the lowest of fuel flows (see Figure 4.14)

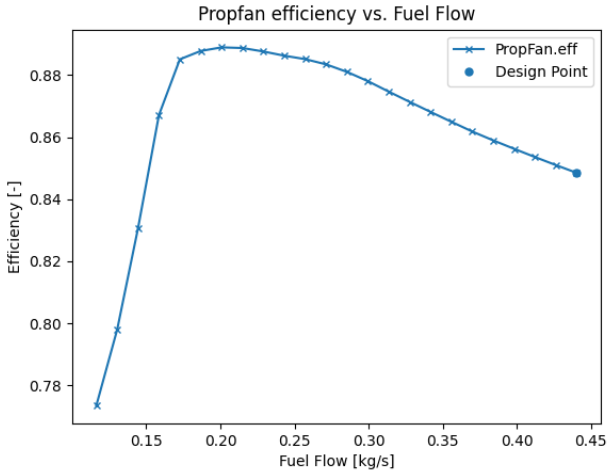

Figure 4.12: Propfan efficiency at cruise conditions for sweep of fuel flow

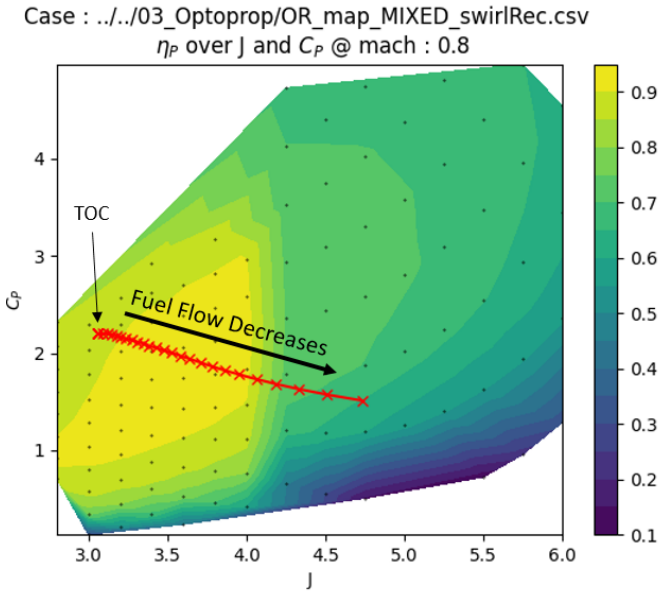

Figure 4.13: Propfan performance map for Mach 0.8. Data set for 100% swirl loss recovery where each data point is shown as a black dot

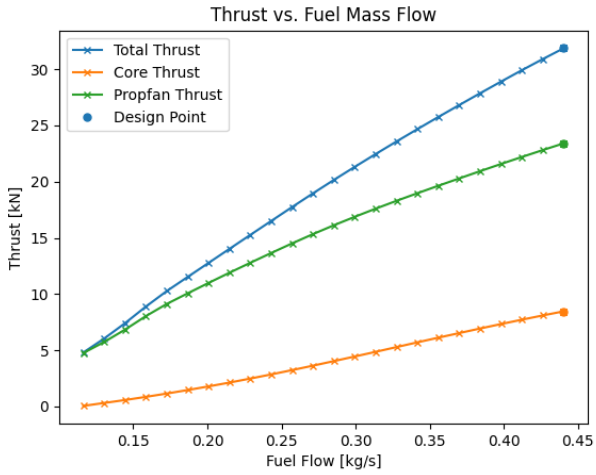

Figure 4.14: Thrust at cruise conditions for sweep of fuel flow

Interesting to note is also that while the power ratio is kept constant a clear shift in how much thrust is generated from the propfan vs. the core of the engine can be seen in Figure 4.14. When plotting this ratio by itself (see Figure 4.15) an almost exponential trend can be seen as the engine is throttled down. This might further explain why the initial approach of setting a fixed thrust ratio lead to poor convergence as keeping the ratio at, as an example, 70% might simply not be possible once the core approaches 0kN net thrust.

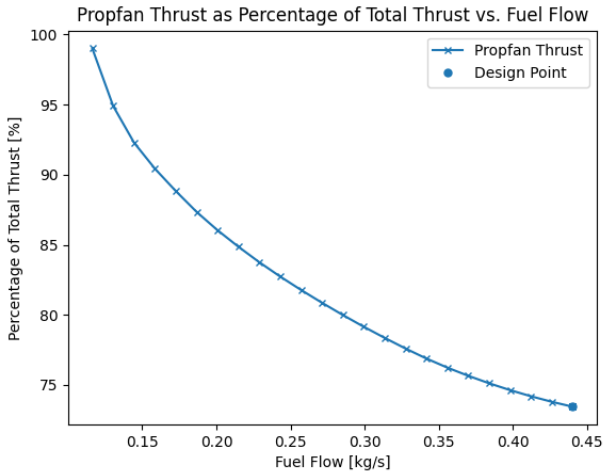

Figure 4.15: Propfan/total thrust ratio at TOC conditions for a sweep of fuel flow

A Brief investigation into the effect of the stall margin on the efficiency was conducted as a response to the findings from the power ratio sweeps. While the range of stall margins that could be investigated was heavily constrained by convergence, a decrease of 33% was possible for both the IPC and LPC SMN. Figure 4.16 shows how a decrease in stall margin does lead to a 1% decrease in SFC during cruise.

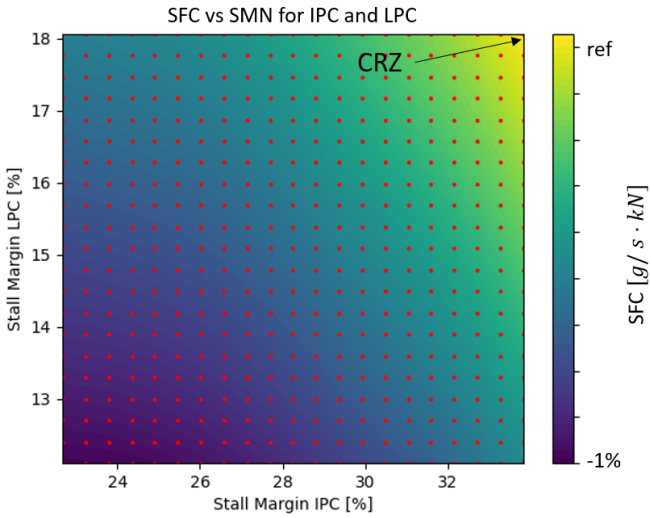

Figure 4.16: A contour of the engines SFC at cruise conditions as a function of SMN for both IPC and LPC

4.3.2 TOEoR

Moving on to looking at the throttling behavior during takeoff conditions. Following a similar trend to what was seen for TOC conditions, we can see that the bleed flow increases as the fuel flow decreases. Different from TOC however is that the engine even at TOEoR the highest looked at fuel flow requires some bleed flow in order to

keep operability. The bleed fraction ends up at around 5% for the LPC and 2.5 for the IPC (see Figure 4.17). As is to be expected from a propeller engine, the SFC ends up significantly lower at TOEoR than at TOC. Comparing the design point SFC to the TOEoR SFC shows an improvement of 32% relative to TOC (see Figure 4.18). When looking at the propfan efficiency we see a different trend than we saw for TOC. Considering the high thrust requirement during take-off one might already have suspected that the efficiency for this condition would be worse compared to TOC since the blade loading would be high and thus C_P high and J low. This is indeed what can be seen in the propfan performance map (see Figure 4.20) and the maximum fuel flow points end up very near the edge of the map data. Plotting this efficiency against fuel flow shows us that the propfan efficiency goes as low as 40% during take-off (see Figure 4.19).

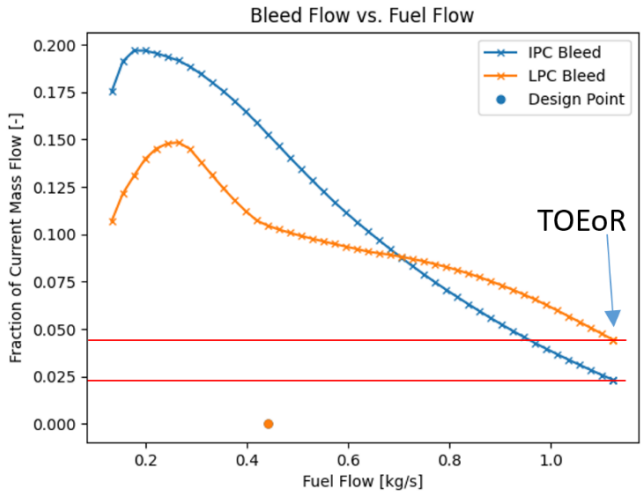

Figure 4.17: Bleed flow at TOEoR conditions for sweep of fuel flow

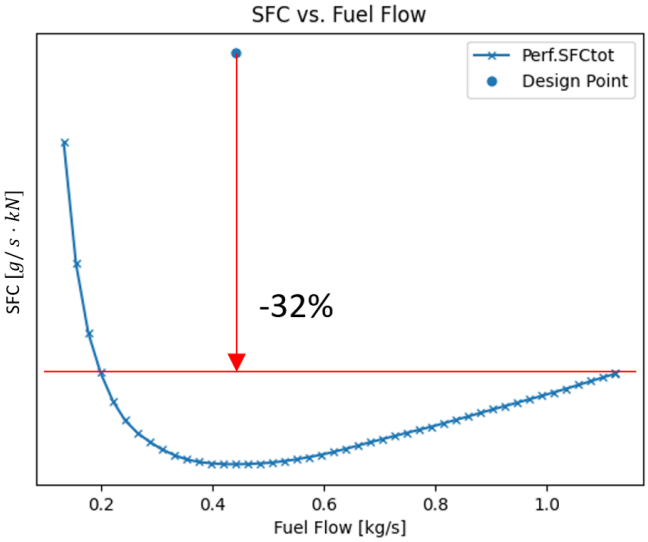

Figure 4.18: SFC at TOEoR conditions for sweep of fuel flow

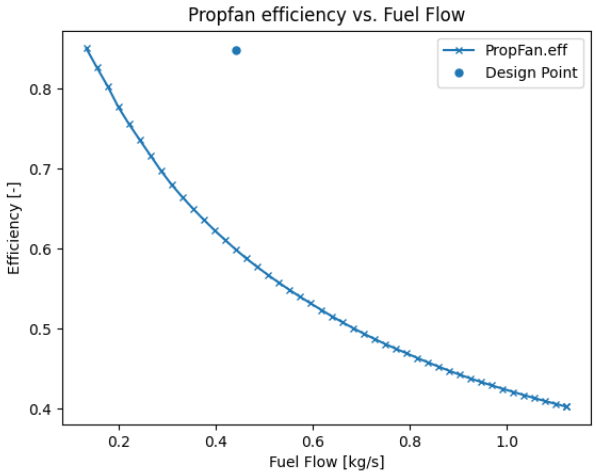

Figure 4.19: Propfan efficiency at TOEoR conditions for sweep of fuel flow

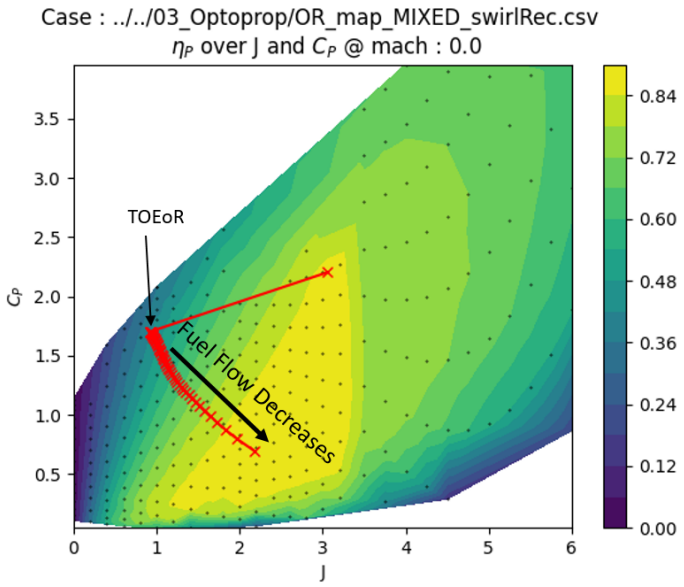

Figure 4.20: Propfan performance map for Mach 0.0. Data set for 100% swirl loss recovery where each data point is shown as a black dot

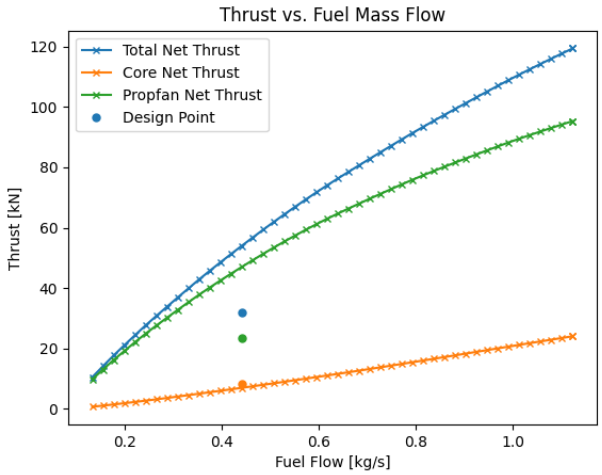

Figure 4.21: Thrust at TOEoR condtions for a sweep of fuel flow

Compared to the TOC condition sweep the TOEoR ends up with a much more linear behaviour in regards to the thrust ratio between the propfan and total thrust. The thrust ratio also remains higher for the entire sweep suggesting that the propfan is as expected working more efficiently at low altitudes and low mach (see Figure 4.22).

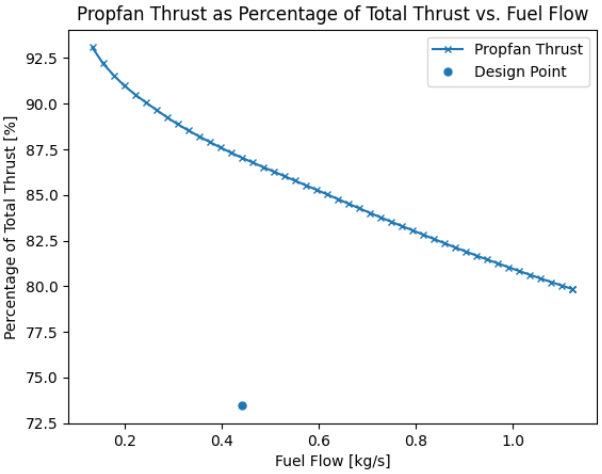

Figure 4.22: Propfan/total thrust ratio at TOEoR conditions for a sweep of fuel flow

4.4 Mission Profile Sweep

In order to verify that the model works for other points than the investigated off-design points a sweep through every point in the provided mission profile was performed. This also served as a good reference as the modeled engine performance could be directly compared to that of the A321.

The efficiency shown in Figure 4.23 is 8-22% better when compared to the original A321 (for climb and cruise). Parts of the descent efficiency can be disregarded due to the 1 kN lower limit set.

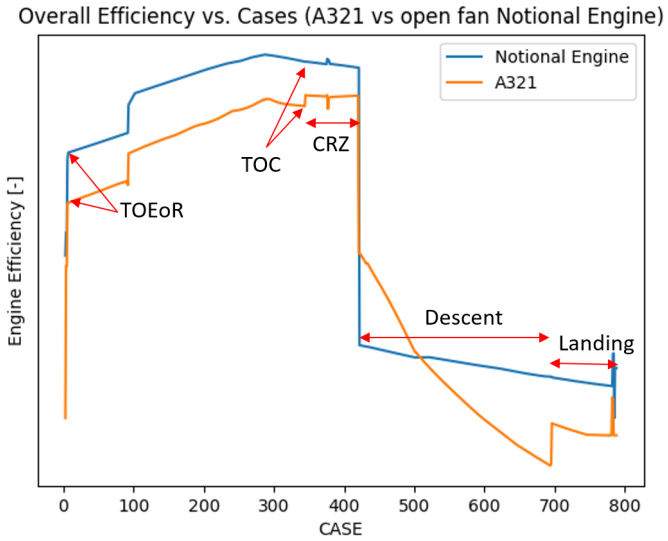

Figure 4.23: Overall engine efficiency for the mission profile sweep, note that the poins are not scaled for time on the x-axis

4.5 Thrust Rating

If we instead sweep through ever increasing fuel flows, in a similar way as described above, we obtain the maximum achievable thrust at each flight condition. This data can be used to formulate a thrust rating for maximum thrust at different altitudes (see Figure 4.24). Note that this is different from the maximum static thrust since the Mach number will vary with the mission profile. However, this makes the data more relevant for the flight envelope since the values more closely reflect the maximum thrust one can expect during flight (see Figure 4.24). Remembering that our take-off thrust requirement was 123 kN, one could propose a flat-rating of 123 kN up to a delta T of +10 K from this data.

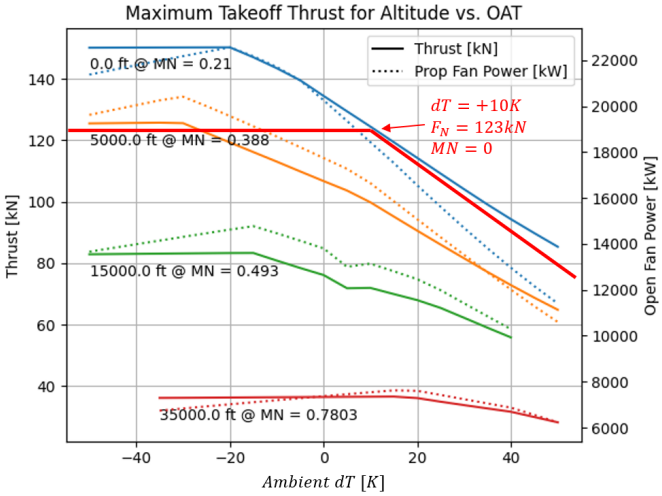

Figure 4.24: Maximum Takeoff thrust rating at a number of points in the mission profile

5
Conclusion and Discussion

In regards to the main objectives of this thesis, it can be concluded that most goals have been looked at in enough detail to give suggestions on how to solve some of the problems one will likely encounter when designing a control scheme for a propfan engine. This includes topics such as operability/stall margin, workload split between the core and propfan, and choice of control variables for thrust scheduling which will be addressed in the following. Following that a general conclusion on the methodology used and the performance will be given.

5.1 Operability and Stall Margin

Very early on it was identified that keeping operability throughout the entire flight envelope would be challenging given the added load the core would need to sustain throughout the mission envelope and throttle regime. While adding a single bleed from the LPC mostly kept the LPC from stalling it did not have a large enough impact on the IPC and HPC to prevent these from reaching and exceeding the stall line. Adding further constraints upon the engine model such as forcing a constant speed stall margin for LPC and IPC prevented the engine from stalling but instead lead to insufficient thrust.

Thus a secondary bleed was added which ultimately solved the issue for the configuration that was used. This made it possible to keep a constant speed stall margin throughout the entire flight envelope including the entire throttle regime. However, using a significant amount of bleed can lead to losses in efficiency so optimising the engine model to require as little bleed as possible for the most used operating conditions (cruise) is important. As mentioned in the results (see Figure 4.10), around 6+% relative bleed mass flow is required at cruise, impacting efficiency for this condition. The brief investigation into varying the stall margin also showed that the selection of the stall margins could have a noticeable impact on the overall engine SFC. As mentioned before however, this model does not model the effect of variable variable IGVs and it is likely that using these could give a similar effect to the current bleed ports without the same loss in efficiency.

It also needs to be mentioned here that using different component maps might lead to vastly different outcomes in regards to keeping operability and investigating the impact of more suitable maps could be of interest for future works.

5.2 Power Ratio and Control Variables

The original design point model used a thrust target for the propfan that was calculated relative to the total thrust target. This approach was kept for off-design initially but gave rise to convergence issues for some cases. Thus, a number of alternate approaches was investigated.

One approach was to keep a fixed shaft spool speed for the low-pressure shaft in order to keep the propfan at a nearly constant tip Mach speed. This approach was inspired by how turboshaft/turboprop engines typically are controlled. This quickly proved to be inefficient given that the spool speed would need to be close to maximum in order to reach TOC and TOEoR thrust requirements but instead be unnecessarily high for cruise and leading to convergence difficulties when reducing the fuel mass flow. This probably is due to the propfan engine differing from a typical turboshaft/turboprop engine by having the propeller connected to the low-pressure shaft and its corresponding components, whereas the latter typically uses a dedicated turbine for the propeller.

In the end, a target ratio between the power used by the propfan and the power generated by the LPT was used as a target value. This led to good convergence for the solver since for a given spool speed there would only be one solution in the propfan map that would match the power ratio and no issues were encountered for cases where the core returned negative net thrust since the produced power by the LPT would remain positive. Figure 4.15 shows how this results in a nonlinear thrust ratio between propfan thrust and total thrust giving some hints as to why the first method might have behaved so poorly for low fuel mass flow conditions. That said, there still is room for improvement in this control scheme, looking at Figure 4.11 shows that the engine's SFC is higher for cruise than for TOC whereas usually for a turbofan the opposite is the case. While varying the power ratio has in this study been found to not help in alleviating this issue, further optimisations in terms of component and propeller performance maps might lead to a different conclusion.

Overall the control strategies investigated here could suggest that contrary to how many turboprop engines are controlled, and propfan engine might not require a two-stick power lever but instead function similarly to a regular turbofan.

5.3 Conclusions on Tools and Methodology

Given that the aim of this thesis was successfully completed with the chosen tools, one cannot argue against these tools at the least being a viable choice. Given that the group's performance, skill, and knowledge with these tools changed significantly during the span of the thesis, a few learning outcomes are worth pointing out.

- Having a flexible and easy-to-use post-processing tool that shows both component maps and line graphs gave a huge boost to the groups understanding and problem-solving capabilities toward the end of the work. Since a significant

part of these tools were built during the span of the thesis one has to consider if the amount of time invested in the creation of these tools was outweighed by their usefulness in the end. For this thesis, the answer would be a clear "yes" given that the tools available at the start of the thesis did not deliver all of the wanted features. Nevertheless, one should in future take this into account when planning projects similar to this one.
- To not underestimate how valuable NPSS' low iteration time is and to use this to one's advantage. Most cases for this model ran in under 1 second per case, this meant that running a grid of 40x40 points in order to get an understanding of which points would converge and which would not only be possible but actually a useful practice leading to contour plots early on that gave a valuable insight into what each variable affected.
- Working on code bases of this size more or less requires the use of some version management software, like Git/Azure. Overall very few issues were encountered with this during the thesis and the possibility to go revert back to a previous "known good" version of the code base proved valuable on multiple occasions.

5.4 Future Work

The implementation of an optimisation loop for stator vanes in addition to the propeller blades for Optoprop has been identifies to be of interest for future evaluations of propfan concepts since this would give a more accurate estimation of the possibility of swirl loss recovery as well as let the user compare the effects of different sizes, shapes and blade profiles for stator vanes. This would however require extensive verification before being viable as a practical tool.

Parts of the stretched target has been out of the timeframe, so these are also a matter of future work. The emissions bookkeeping in NPSS could be used as a further improving the propfan concept.

Running the model in a transient state within the mission envelope could be beneficial to see how other mission points compare to other aero engines. This can also be beneficial to see the effects of inertia of the propeller, the effects of spooling up and down both the inner core and the propeller. This would require a more simulation time and might require some additional adaptation of the propfan specific element.

A lot of optimization work would also be relevant to complete to get the most out of the propfan engine. In this it could be included to further investigate optimisation of the power ratio between the propfan and low speed shaft as well as alternate component layouts.

Installation effects were not considered so far in this work, but as seen in other reports the installation effects can have an impact on the results. This could also be one of the points to consider when improving and rerunning simulations.

As stated previously the variable IGVs for each stage are not modelled. However, it is shown in other works that they can reduce bleed air, which would improve performance, SFC and efficiency. Implementing an IGV element in NPSS or adding this functionality to the existing compressor elements might be of interest. [25]

Somewhat connected to the previous idea, is the possibility of investigating other component maps since the component sizing, while not investigated in this thesis, could differ from a typical turbofan and as such require component maps more suitable for this application. This could also include taking into account the flow acceleration from the propeller and the effect this could have on the LPC given the suspected slight increase in pressure.

Finally, while a proposal for a thrust rating strategy has been given in this thesis, a more concrete investigation into the scheduling and mapping of all the proposed variables against PLA could be of interest in comparing how the operation of a propfan engine might differ from a turbofan.

Bibliography

[1] I. A. T. Association. "Our commitment to fly net zero by 2050."
(Feb. 2023),
[Online]. Available: `https://www.iata.org/en/programs/environment/flynetzero/`.

[2] L. Larsson, A. Lundbladh, and T. Grönstedt,
"Effects of different propeller models on open rotor fuel consumption,"
In *International Society for Airbreathing Engines, ISABE, Busan, South Korea, 2013*,
2013.

[3] L. Billman, C. Gruska, R. Ladden, D. Leishman, and J. Turnberg,
"Large scale prop-fan structural design study. volume 2: Preliminary design of sr-7,"
Tech. Rep.,
1988.

[4] R. D. Hager,
Advanced turboprop project.
Scientific and Technical Information Division, National Aeronautics and ...,
1988,
Vol. 495.

[5] J. Godston and C. Reynolds,
"Future prop-fans-tractor or pusher,"
In *21st Joint Propulsion Conference*,
1985,
P. 1189.

[6] D. F. Sarglsson,
Advanced propfan engine technology (apet) and single-rotation gearbox/ pitch change mechanism,
1985.

[7] D. Chapman, J. Godston, and D. Smith,
"Testing of the 578-dx propfan propulsion system,"
In *24th Joint Propulsion Conference*,
1988,

P. 2804.

[8] D. E. Van Zante,
"Progress in open rotor research: A us perspective,"
In *Turbo Expo: Power for Land, Sea, and Air*,
American Society of Mechanical Engineers,
Vol. 56628, 2015,
V001T01A003.

[9] *Jet engines basic*,
BOEING, 2003.
[Online]. Available: `https://www.smartcockpit.com/docs/Jet_Engines_Basics.pdf`.

[10] J. Baum, P. Dumais, M. Mayo, F. Metzger, A. Shenkman, and G. Walker,
"Prop-fan data support study,"
Tech. Rep.,
1978.

[11] I. J. Sandra Busch,
Wind tunnel test of a double blade swept propeller and analysis of real geometry effects,
2015.

[12] M. I. of Technology. "11.7 mit performance of propellers."
(Jun. 2023),
[Online]. Available: `https://web.mit.edu/16.unified/www/FALL/thermodynamics/notes/node86.html`.

[13] C. Miller,
"Euler analysis of a swirl recovery vane design for use with an advanced single-rotation propfan,"
In *24th Joint Propulsion Conference*,
1988,
P. 3152.

[14] D. Raymer,
Aircraft design: a conceptual approach.
American Institute of Aeronautics and Astronautics, Inc., 2012.

[15] T. Saeed, W. Graham, H. Babinsky, *et al.*,
"Conceptual design for a laminar flying wing aircraft,"
In *27th AIAA Applied Aerodynamics Conference*,
2009,
P. 3616.

[16] P. Alves, M. Silvestre, and P. Gamboa, "Aircraft propellers—is there a future?"
Energies, vol. 13, no. 16, p. 4157, 2020.

[17] J. Kurzke,
"Modeling the thrust management of commercial airliners,"
In *International Symposium on Air Breathing Engine*,
2013.

[18] *As681 rev k*,
SAE International, 2016.

[19] P. Gupta, "Advanced olympus for next generation supersonic transport aircraft,"
SAE Transactions, pp. 2265–2289, 1980.

[20] N. E. Daidzic, "Jet engine thrust ratings,"
Professional Pilot, vol. 46, no. 9, 2012.

[21] *Getting to grips with, aircraft performance*,
Airbus, Airbus, Jan. 2002.

[22] R. Irsyadi and W. Nirbito,
"Derated thrust: Method analysis for optimizing turbofan engine takeoff performances (sfc, egt) due to lower maximum takeoff weight (mtow) requirement,"
In *IOP Conference Series: Materials Science and Engineering*,
IOP Publishing,
Vol. 685, 2019,
P. 012 007.

[23] M. I. of Technology. "Mit 11.1 multistage axial compressors."
(Jun. 2023),
[Online]. Available: `https://web.mit.edu/16.unified/www/FALL/thermodynamics/notes/node80.html`.

[24] M. I. of Technology. "Mit 12.4 multistage axial compressors."
(Jun. 2023),
[Online]. Available: `https://web.mit.edu/16.unified/www/FALL/thermodynamics/notes/node92.html`.

[25] N. A. Cumpsty, "Compressor aerodynamics,"
Longman Scientific & Technical, 1989.

[26] J. D. Brooks,
"A methodology for capturing the impacts of bleed flow extraction on compressor performance and operability in engine conceptual design,"
Ph.D. dissertation, Georgia Institute of Technology, 2015.

[27] NASA. "Power turbine."
(Jun. 2023),
[Online]. Available: `https://www.grc.nasa.gov/www/k-12/airplane/powturb.html`.

[28] S. L. Dixon and C. Hall,
Fluid mechanics and thermodynamics of turbomachinery.
Butterworth-Heinemann, 2013.

[29] P. P. Walsh and P. Fletcher,
Gas turbine performance.
John Wiley & Sons, 2004.

[30] H. I. Saravanamuttoo, G. F. C. Rogers, and H. Cohen,
Gas Turbine Theory seventh edition.
Pearson Education Limited, 2017.

[31] *Introduction to propulsion simulation using npss*,
Southwest Research Institute, Southwest Research Institute, 2018.

[32] A. C. Patrao,
On the aerodynamic design of the boxprop.
Chalmers Tekniska Hogskola (Sweden), 2018.

[33] *Specification and description king air 350i*,
Beechcraft, Textron aviation, Oct. 2015.

DEPARTMENT OF MECHANICS AND MARITIME SCIENCES
CHALMERS UNIVERSITY OF TECHNOLOGY
Gothenburg, Sweden
www.chalmers.se

CHALMERS
UNIVERSITY OF TECHNOLOGY